IOPscience iopscience.iop.org

Home Search Collections Journals About Contact us My IOPscience

The nature of the atomic surfaces of quasiperiodic self-similar structures

This article has been downloaded from IOPscience. Please scroll down to see the full text article.

1993 J. Phys. A: Math. Gen. 26 1951

(http://iopscience.iop.org/0305-4470/26/8/020)

View the table of contents for this issue, or go to the journal homepage for more

Download details:
IP Address: 171.66.16.68
The article was downloaded on 01/06/2010 at 21:11

Please note that terms and conditions apply.

J. Phys. A: Math. Gen. 26 (1993) 1951–1999. Printed in the UK

The nature of the atomic surfaces of quasiperiodic self-similar structures

J M Luck†‡, C Godrèche‡§, A Jannert‡ and T Janssen‡

† Service de Physique Théorique*, Centre d'Études de Saclay, 91191 Gif-sur-Yvette cedex, France

‡ Institute for Theoretical Physics, University of Nijmegen, Toernooiveld 1, 6525 ED Nijmegen, The Netherlands

§ Service de Physique de l'État Condensé*, Centre d'Études de Saclay, 91191 Gif-sur-Yvette cedex, France

Received 14 September 1992

Abstract. Quasiperiodic self-similar chains generated by substitutions (i.e. deterministic concatenation rules) and their diffraction spectra are analysed in a systematic fashion, from the viewpoint of the superspace formalism. A substitution acting on n objects generates quasiperiodic chains if, and only if, the associated substitution matrix fulfils two arithmetic conditions (Pisot property and unit determinant). The structures thus obtained can be alternatively built as sections of periodic patterns in an n-dimensional superspace, which are regular repetitions of an atomic surface. We derive a general algorithm to construct this atomic surface. It is a compact set of the $(n-1)$-dimensional internal space, which is a unit cell for a lattice of translations. The atomic surface is nevertheless not necessarily connected, and its boundary is generically an anisotropic self-similar fractal. The dimension d_B of this boundary is shown to govern the anomalously slow fall-off of the intensities of Bragg diffractions, and therefore to influence physical properties.

1. Introduction

There are two well known approaches to the construction of quasiperiodic tilings. Historically, the first aperiodic tilings of the plane, such as those of Penrose and Ammann [1], were described by 'inflation rules', which were applied iteratively to the tiles. The one-dimensional Fibonacci chain provides a simple illustration of this procedure, alternatively called 'substitution' or 'concatenation'. One is given two letters, A and B, and one substitutes AB for A, and A for B. One then associates bond lengths ℓ^A, ℓ^B, to each letter type. The second approach, namely the cut-and-project or section method, describes a two- or three-dimensional tiling by means of a higher-dimensional space. As a matter of fact, this way of visualising quasiperiodic structures in 'superspace' had already been introduced for incommensurate structures [2]. It is indeed both natural and economical to view a quasiperiodic structure in d-dimensional 'physical space' as the section of a periodic object in an n-dimensional superspace, with $n > d$. For instance, when dealing with a

* Laboratoires de la Direction des Sciences de la Matière du Commissariat à l'Énergie Atomique.

0305-4470/93/081951+49$07.50 © 1993 IOP Publishing Ltd

quasiperiodic tiling, it is advantageous to book-keep vertex positions as sets of integer coordinates in superspace.

These two approaches are quite different. Indeed, the nature of the diffraction spectrum, i.e. of the Fourier transform, of the aperiodic structures obtained with the first one is unknown *a priori*, whereas, from its very definition, the second one produces quasiperiodic objects, characterized the fact that their Fourier transform consists of Bragg peaks, i.e. delta functions, supported by a module over the integers, spanned by n basis vectors in reciprocal space. Many systems share this property [3], among which there are incommensurate modulated crystal phases, incommensurate composite (misfit) structures, helicoidal magnetic structures, and quasicrystals.

Taking some distance, the following question is to be raised. Whereas the second method automatically generates quasiperiodic objects, one is led to wonder what kind of Fourier spectrum corresponds to structures generated by substitution rules, and, more generally, what is the relationship between long-range order and the self-similarity implied by inflation or substitution rules. It is worth noticing the difference between these two ways of characterizing 'regularity' or 'symmetry'. The long-range order coded in a diffraction spectrum corresponds to regularity properties with respect to translations, whereas inflation symmetry is linked with discrete dilatations. Both are 'repetitions', but not of the same kind. Bombieri and Taylor [4] produced the following criterion, in the case of one-dimensional structures: whenever a substitution has the Pisot property, defined below, the associated structure possesses Bragg peaks. Conversely, non-Pisot structures usually exhibit complex diffraction spectra [5–9] with singular scattering peaks, and multifractal scaling properties.

Let us restrict the analysis to Pisot structures, and thus to Bragg diffraction spectra. Under the extra hypothesis, again to be discussed below, that the substitution matrix has unit determinant, a quasiperiodic object is generated, which can be embedded in a transversally bounded strip of a higher-dimensional superspace. In other words, it is possible to generate the structure by a section method, from a periodic array of bounded 'atomic surfaces'. We recall that a quasiperiodic structure in d dimensions may be obtained as the intersection of a d-dimensional physical space V^{E} with a periodic structure in an n-dimensional superspace, where $n > d$ is the rank of the Fourier module mentioned above [2, 10, 11]. If Λ is the lattice of periods of the superspace structure, and if Λ^* denotes its reciprocal lattice, then the Fourier module of the structure is some projection of Λ^* onto V^{E} [3]. For quasiperiodic tilings, the superspace structure is a periodic array of atomic surfaces, which are bounded $(n-d)$-dimensional domains, included in 'internal space' V^{I}, which is complementary to physical space [12–14]. Moreover, in the case of substitutional structures, n is generically equal to the number of 'letters' involved by the substitution rules, e.g. $n = 2$ for the Fibonacci chain. In other words, substitutional chains can be viewed as incommensurately modulated displacive structures, with a periodic chain as basic structure. Finally, under certain conditions on the bond lengths, to be specified later on, the existence of a substitution leads to an exact scale invariance of the corresponding quasiperiodic structures; this geometrical self-similarity plays a role in the study of their physical properties [15].

At least in one dimension, there are infinitely many quasiperiodic structures, built from substitutions. One may therefore wonder what is the superspace description of all those structures (as recalled above, this is the natural framework to describe them). The answer could have been simple, namely that every quasiperiodic structure corresponds to regular atomic surfaces. We soon discovered, to our surprise, that

a *generic* one-dimensional quasiperiodic substitutional structure leads to a complex atomic surface, with a fractal boundary. We should mention that fractal atomic surfaces had already been mentioned for some instances of tilings [16].

The description of this phenomenon, and its full quantitative explanation, represent the aim of this paper. Both the ideas and the formalism exposed below will be extended to tilings of the plane in a separate publication. Since this work comes as the latest of a long list, we chose to write it in a self-contained way, in order for the reader to avoid the tedious task of searching for definitions through previous publications. Hence some parts contain material already published elsewhere; we also want to apologize for the unavoidable numerous self-quotations.

This paper is organised as follows. Section 2 is devoted to a description of chains generated by binary substitutions. We give a systematic account, with some generalization, of the main outcomes of previous works, thus producing a self-contained summary of concepts and notations. section 3 contains the heart of the paper, namely the description of how to construct the atomic surface of any quasiperiodic substitutional chain, taking the binary example for definiteness. In section 4 we study several examples of binary chains. Section 5 is devoted to a generalization of previous results to substitutions acting on more than two letters, with examples of ternary chains. A brief conclusion is presented in section 6. Two appendices contain more technical material, namely a derivation of the Fourier module in the general case, and the investigation of a binary Cantor function, which helps understanding the properties of atomic surfaces with fractal boundaries.

2. Binary chains: general formalism

In this section, we present a self-contained overview of general results concerning the structures generated by binary substitutions, their geometrical characteristics, and the nature of their diffraction spectrum.

2.1. Binary substitutions and structures

A binary substitution σ is formally defined by its action on an alphabet $\mathcal{A} = \{A, B\}$, which consists of two letters. The substitution replaces each letter by a finite word, of the form

$$\sigma : \begin{cases} A \to \sigma(A) = a_1 \dots a_{\alpha+\beta} \\ B \to \sigma(B) = b_1 \dots b_{\gamma+\delta} \,. \end{cases} \tag{2.1}$$

In the expression (2.1), each a_i or b_i stands for a letter, which is either A or B, and α, β, γ, and δ are four positive integers, which denote the numbers of letters of each type in the words $\sigma(A)$ and $\sigma(B)$. It is useful to recast these numbers in the form of a 2×2 integer matrix M, called the substitution matrix associated with σ, and defined as follows:

$$\mathsf{M} = \begin{pmatrix} \alpha & \gamma \\ \beta & \delta \end{pmatrix} = \begin{pmatrix} \text{number of } A\text{s in } \sigma(A) & \text{number of } A\text{s in } \sigma(B) \\ \text{number of } B\text{s in } \sigma(A) & \text{number of } B\text{s in } \sigma(B) \end{pmatrix} . \tag{2.2}$$

The substitution matrix therefore only describes the contents of the words $\sigma(A)$ and $\sigma(B)$ in letters of each type, irrespective of the order in which these letters occur. In

particular, two substitutions that only differ by the ordering of letters have identical matrices.

We define the sequence of words A_n and B_n, obtained by acting repeatedly with the substitution σ on the letters A and B:

$$A_n = \sigma^n(A) \qquad B_n = \sigma^n(B)\,. \tag{2.3}$$

The substitution matrix M permits the evaluation of the total numbers of letters contained in the words A_n and B_n, denoted respectively ν_n^A and ν_n^B. We have indeed

$$\begin{pmatrix} \nu_{n+1}^A \\ \nu_{n+1}^B \end{pmatrix} = \mathsf{M}^T \begin{pmatrix} \nu_n^A \\ \nu_n^B \end{pmatrix} \tag{2.4}$$

and therefore

$$\begin{pmatrix} \nu_n^A \\ \nu_n^B \end{pmatrix} = (\mathsf{M}^T)^n \begin{pmatrix} 1 \\ 1 \end{pmatrix} \tag{2.5}$$

where M^T denotes the transpose of the matrix M.

In order to work out the result (2.5) in closed form, we have to determine the spectrum of the substitution matrix M, which will play a central role throughout the following. Its characteristic polynomial reads

$$P(\lambda) = \det(\lambda 1 - \mathsf{M}) = \lambda^2 - s\lambda + p = (\lambda - \lambda_1)(\lambda - \lambda_2)\,. \tag{2.6}$$

In this expression,

$$s = \operatorname{tr}\mathsf{M} = \alpha + \delta \qquad p = \det\mathsf{M} = \alpha\delta - \beta\gamma \tag{2.7}$$

are the invariants of the substitution matrix M, and

$$\lambda_1 = \frac{s + \sqrt{\Delta}}{2} \qquad \lambda_2 = \frac{s - \sqrt{\Delta}}{2} \qquad \text{with} \qquad \Delta = s^2 - 4p = (\alpha - \delta)^2 + 4\beta\gamma \tag{2.8}$$

are its eigenvalues.

We also define a sequence of integers Φ_n, through the recursion formula

$$\Phi_n = s\Phi_{n-1} - p\Phi_{n-2} \tag{2.9}$$

with $\Phi_0 = 0$, $\Phi_1 = 1$, and where s and p are the invariants defined in (2.7). We thus have $\Phi_2 = s$, $\Phi_3 = s^2 - p$, and so on.

These integers and the eigenvalues of the matrix M are related through the identities

$$\Phi_n = \frac{\lambda_1^n - \lambda_2^n}{\lambda_1 - \lambda_2} \qquad \lambda_1^n = \Phi_{n+1} - \lambda_2\Phi_n \qquad \lambda_2^n = \Phi_{n+1} - \lambda_1\Phi_n \tag{2.10}$$

which allow us to evaluate the successive powers of the substitution matrix in closed form. We thus obtain

$$\mathsf{M}^n = \begin{pmatrix} \Phi_{n+1} - \delta\Phi_n & \gamma\Phi_n \\ \beta\Phi_n & \Phi_{n+1} - \alpha\Phi_n \end{pmatrix}. \tag{2.11}$$

The total letter numbers of the words A_n and B_n can then be derived from (2.5) as

$$\nu_n^A = \Phi_{n+1} + (\beta - \delta)\Phi_n \qquad \nu_n^B = \Phi_{n+1} + (\gamma - \alpha)\Phi_n \,. \tag{2.12}$$

We assume in the following that $\sigma(A)$ begins with the letter A, and that the substitution matrix $\mathbf{M}$ is primitive [17]. This means that all entries of $\mathbf{M}^N$ are strictly positive integers, for some integer $N \geqslant 1$. Under these conditions, the sequence of words A_n converges toward a semi-infinite sequence $\Sigma = \sigma^\infty(A)$, such that $\Sigma = \sigma(\Sigma)$. We have thus obtained an infinite abstract sequence which is self-similar.

Under the above conditions, the Perron–Frobenius theorem asserts that the eigenvalue with larger modulus, say λ_1, is real, positive, and larger than one (see e.g. [18]). In the binary case under consideration, λ_2 is also real. The right eigenvector $\mathbf{v}_1$ of $\mathbf{M}$, associated with λ_1, reads

$$\mathbf{v}_1 = \begin{pmatrix} \rho^A \\ \rho^B \end{pmatrix}$$
$$\rho^A = \frac{\gamma}{\lambda_1 + \gamma - \alpha} = \frac{\lambda_1 - \delta}{\lambda_1 + \beta - \delta} \qquad \rho^B = \frac{\lambda_1 - \alpha}{\lambda_1 + \gamma - \alpha} = \frac{\beta}{\lambda_1 + \beta - \delta} \,. \tag{2.13}$$

These components, which are positive and normalized so that $\rho^A + \rho^B = 1$, are the frequencies, or densities, of the letters A and B in the infinite sequence Σ.

Before we proceed, let us exemplify the above definitions with the simple case of the Fibonacci substitution

$$\sigma_{\mathrm{F}} : \begin{vmatrix} A \to AB \\ B \to A. \end{vmatrix} \tag{2.14}$$

The associated substitution matrix reads

$$\mathbf{M} = \begin{pmatrix} 1 & 1 \\ 1 & 0 \end{pmatrix} \tag{2.15}$$

and its eigenvalues are $\lambda_1 = \tau$, $\lambda_2 = -\tau^{-1}$, where

$$\tau = \frac{1 + \sqrt{5}}{2} = 1.618\,034 \tag{2.16}$$

is the golden mean. The integers Φ_n coincide with the Fibonacci numbers F_n, defined by the following recursion relation:

$$F_n = F_{n-1} + F_{n-2} \qquad F_0 = 0 \quad F_1 = 1 \,. \tag{2.17}$$

There are several ways of associating a geometrical structure with an infinite abstract sequence such as Σ. One simple choice [5–7,9] consists in viewing A and B as beads with two different sizes, which we string along a thread in an ordered fashion. More precisely, we associate two arbitrary (positive) bond lengths ℓ^A, ℓ^B to the letters, and we place pointlike atoms on a line, at abscissas x_k such that $x_0 = 0$, and the kth bond length

$$\ell_k = x_k - x_{k-1} \qquad k \geqslant 1 \tag{2.18}$$

is chosen according to $\ell_k = \ell^A$ (respectively, $\ell_k = \ell^B$), if the kth letter of the sequence Σ is an A (respectively, a B). As a consequence, the mean interatomic distance, or inverse density, of the structure reads

$$a = \lim_{k\to\infty} \frac{x_k}{k} = \rho^A \ell^A + \rho^B \ell^B \,. \tag{2.19}$$

Let us consider the words A_n and B_n, defined in (2.3), and denote the lengths of the associated structures by ℓ_n^A and ℓ_n^B. These quantities obey the same linear recursion relations (2.4) as the numbers of letters. We have therefore

$$\ell_n^A = (\Phi_{n+1} - \delta\Phi_n)\ell^A + \beta\Phi_n \ell^B \qquad \ell_n^B = \gamma\Phi_n \ell^A + (\Phi_{n+1} - \alpha\Phi_n)\ell^B \,. \tag{2.20}$$

The dimensionless ratio ℓ^A/ℓ^B of both bond lengths is an arbitrary parameter. There is nevertheless a natural choice for this quantity, which will be given a simple geometrical interpretation in the next section. For the time being, consider the ratios ξ_n between the total lengths of the words A_n and B_n

$$\xi_n = \frac{\ell_n^A}{\ell_n^B} \,. \tag{2.21}$$

We have the following mapping T_σ between successive ratios:

$$\xi_{n+1} = T_\sigma(\xi_n) = \frac{\alpha\xi_n + \beta}{\gamma\xi_n + \delta} \,. \tag{2.22}$$

When the generation label n becomes large, the ratios ξ_n converge toward the attractive fixed point ξ_* of this map, which reads

$$\xi_* = \frac{\beta}{\lambda_1 - \alpha} = \frac{\lambda_1 - \delta}{\gamma} \,. \tag{2.23}$$

In the following, we assume that the initial ratio of both bond lengths assumes its fixed-point value

$$\xi_0 = \frac{\ell^A}{\ell^B} = \xi_* \,. \tag{2.24}$$

Under this condition, the bond lengths and the atomic spacing are related through

$$\ell^A = \frac{\lambda_1 + \beta - \delta}{\lambda_1 - \lambda_2}\, a \qquad \ell^B = \frac{\lambda_1 + \gamma - \alpha}{\lambda_1 - \lambda_2}\, a \tag{2.25}$$

and the total lengths of the words A_n and B_n read

$$\ell_n^A = \lambda_1^n \, \ell^A \qquad \ell_n^B = \lambda_1^n \, \ell^B \,. \tag{2.26}$$

We end up by noticing that the fixed-point condition (2.24) amounts to requiring that the bond lengths are proportional to the components of the left Perron–Frobenius eigenvector w_1 of the substitution matrix M, associated with the eigenvalue λ_1.

2.2. Superspace representation

An alternative way of viewing the substitutional structure defined above consists in embedding it into a two-dimensional superspace. Let $\{e_1, e_2\}$ denote a basis of a lattice in two dimensions, with no metric structure *a priori*. We define an infinite sequence of lattice points X_k through $X_0 = 0$, and so that the vector difference

$$L_k = X_k - X_{k-1} \qquad k \geqslant 1 \tag{2.27}$$

is chosen according to $L_k = e_1$ (respectively, $L_k = e_2$), if the kth bond of the structure has length ℓ^A (respectively, ℓ^B), i.e. if the kth letter of the sequence Σ is an A (respectively, a B). We have therefore

$$X_k = m^A(k)e_1 + m^B(k)e_2 \tag{2.28}$$

where the integers $m^A(k)$ and $m^B(k)$ are respectively the numbers of letters A and B among the first k letters of the sequence Σ. These numbers obey the evident sum rule

$$m^A(k) + m^B(k) = k\,. \tag{2.29}$$

We thus obtain an infinite staircase-shaped broken line, drawn on the lattice, which escapes to infinity along the mean direction of the vector

$$v_1 = \lim_{k\to\infty} \frac{X_k}{k} = \rho^A e_1 + \rho^B e_2 \tag{2.30}$$

coinciding with the definition (2.13).

Let us call *physical space*, and denote by V^{E}, the real linear space spanned by the vector v_1. V^{E} is thus the eigenspace of the substitution matrix M, associated with the Perron–Frobenius eigenvalue λ_1. Along the same lines, we call *internal space*, and we denote by V^{I}, the eigenspace of M, associated with the second eigenvalue λ_2. This linear space is spanned by a vector v_2 given by

$$v_2 = \begin{pmatrix} \eta^A \\ \eta^B \end{pmatrix} \qquad \text{with} \qquad \eta^A = \frac{\gamma + \delta - \lambda_2}{\lambda_1 - \lambda_2} \qquad \eta^B = \frac{\lambda_2 - \alpha - \beta}{\lambda_1 - \lambda_2}\,. \tag{2.31}$$

We define the dimensionless fluctuations u_k of the atomic abscissas x_k, with respect to the average lattice of the structure, as follows:

$$x_k = m^A(k)\ell^A + m^B(k)\ell^B = ka + (\ell^A - \ell^B)u_k\,. \tag{2.32}$$

The second of these equalities, together with the sum rule (2.29), yields

$$m^A(k) = k\rho^A + u_k \qquad m^B(k) = k\rho^B - u_k\,. \tag{2.33}$$

We denote by X_k^{E} and X_k^{I} the projections of the vector X_k onto physical and internal spaces, defined by

$$X_k = X_k^{\mathrm{E}}\, v_1 + X_k^{\mathrm{I}}\, v_2\,. \tag{2.34}$$

These quantities can be expressed in terms of the fluctuations u_k as follows:

$$X_k^{\mathrm{E}} = k + \frac{\alpha + \beta - \gamma - \delta}{\lambda_1 - \lambda_2} u_k \qquad X_k^{\mathrm{I}} = u_k \,. \tag{2.35}$$

The second of these equalities is a consequence of the choice of normalization of the vector v_2, made in (2.31). The first of them allows us to check that the atomic abscissas x_k are proportional to the projections X_k^{E} if, and only if, the ratio between both bond lengths ℓ^A and ℓ^B assumes its fixed-point value, determined in (2.23). This is indeed the condition under which the substitution acts on the physical structure exactly as a dilatation by the scaling factor λ_1, so that the structure is strictly self-similar, and can be viewed as a linear projection of the staircase-shaped broken line onto the physical space V^{E}.

2.3. Extension in internal space

The result (2.35) shows that the internal coordinates X_k^{I} of the atoms coincide with the fluctuations u_k of the structure with respect to its average lattice. This section is devoted to the asymptotic long-distance behaviour of these fluctuations ($k \to \infty$).

In order to get an estimate of the fluctuations, let us focus our attention on the finite samples of the structure associated with the words A_n and B_n, introduced in (2.3). The total letter numbers and the lengths of these pieces have been determined in (2.12) and (2.20), respectively, in terms of the integers Φ_n.

The associated fluctuations, defined in analogy with (2.32), read

$$u_n^A = \frac{\ell_n^A - \nu_n^A a}{\ell^A - \ell^B} = \frac{\beta}{\lambda_1 + \beta - \delta} \lambda_2^n \qquad u_n^B = \frac{\ell_n^B - \nu_n^B a}{\ell^A - \ell^B} = -\frac{\gamma}{\lambda_1 + \gamma - \alpha} \lambda_2^n \,. \tag{2.36}$$

Two cases have therefore to be considered, according to the magnitude of $|\lambda_2|$ with respect to unity. Whenever we have $|\lambda_2| < 1$, we shall say that the substitution σ, and the associated matrix **M**, have the *Pisot–Vijayaraghavan property*, called *Pisot property* for short in the following.

This term originates in the following definition. A *Pisot–Vijayaraghavan number* [19, 20] is a real number $x > 1$, which is an algebraic integer of any degree $m \geqslant 1$, i.e. the solution of a polynomial equation of the form $Q(x) = x^m + a_{m-1}x^{m-1} + \cdots + a_0 = 0$, where the a_k are integers, such that all its conjugates, namely the other $(m-1)$ real or complex roots of the equation $Q(x) = 0$, are smaller than unity in modulus. The above definition of a Pisot substitution σ amounts to saying that the Perron–Frobenius eigenvalue λ_1 is a Pisot number, under the condition that the characteristic polynomial $P(\lambda)$, evaluated in (2.6), is irreducible over the integers.

(i) If the substitution has the Pisot property ($|\lambda_2| < 1$), the estimate (2.36) shows that the fluctuations associated with the words A_n and B_n go to zero exponentially with n. It turns out that the fluctuations u_k are bounded, for all values of the atomic label k.

(ii) If the substitution does not have the Pisot property ($|\lambda_2| \geqslant 1$), the fluctuations of the words A_n and B_n diverge as λ_2^n, whereas the system sizes diverge as λ_1^n. This observation suggests that the fluctuations u_k obey the following power law:

$$u_k \sim k^{\zeta} \qquad \text{with} \qquad \zeta = \frac{\ln |\lambda_2|}{\ln \lambda_1} \,. \tag{2.37}$$

The 'wandering exponent' ζ is such that $0 < \zeta < 1$. The above estimate has been turned into a rigorous argument [17], which yields the more accurate asymptotic scaling law

$$u_k \approx k^{\zeta} G\left(\frac{\ln k}{\ln \lambda_1}\right) \tag{2.38}$$

where the amplitude G is a periodic function of its argument $z = \ln k / \ln \lambda_1$, with unit period. The oscillatory amplitude G is generically a fractal function, which is continuous, but nowhere differentiable.

In the marginal case where $\lambda_2 = \pm 1$, the fluctuations diverge only logarithmically. Examples of this situation have been examined in [5,6,21].

2.4. Nature of the diffraction spectrum

We show in this section that the nature of the diffraction spectrum of a substitutional structure is also dictated by the eigenvalues of the associated substitution matrix, and especially by its Pisot character. The diffraction spectrum of a structure is the Fourier transform of some mass distribution living on the structure. For the sake of simplicity, we choose to put identical pointlike atoms at the abscissas $\{x_k\}$.

In order to investigate the associated diffraction spectrum, we consider the Fourier amplitudes corresponding to the finite words A_n and B_n, defined as

$$G_n^A(Q) = \sum_{x_k \in A_n} \mathrm{e}^{-\mathrm{i}Qx_k} \qquad G_n^B(Q) = \sum_{x_k \in B_n} \mathrm{e}^{-\mathrm{i}Qx_k} \tag{2.39}$$

where Q is an arbitrary one-dimensional wavevector. These Fourier amplitudes obey recursion formulae, which express the iterative definition (2.3) of the words themselves. Taking the example of the Fibonacci substitution (2.14) for definiteness, we obtain

$$G_{n+1}^A(Q) = G_n^A(Q) + \exp\left(-\mathrm{i}Q\ell_n^A\right) G_n^B(Q) \qquad G_{n+1}^B(Q) = G_n^A(Q)\,. \tag{2.40}$$

In these equations, the phase factor involves the lengths of the words A_n, which have been evaluated in (2.20). The formulae (2.40), with the initial conditions $G_0^A(Q) = \exp(-\mathrm{i}Q\ell^A)$, $G_0^B(Q) = \exp(-\mathrm{i}Q\ell^B)$, determine entirely the Fourier amplitudes. They allow therefore the evaluation of the structure factor, or Fourier intensity, $S(Q)$, associated with the infinite structure, which is formally defined as the limit

$$S(Q) = \lim_{n\to\infty} \frac{\left|G_n^A(Q)\right|^2}{\nu_n^A} = \lim_{n\to\infty} \frac{\left|G_n^B(Q)\right|^2}{\nu_n^B}\,. \tag{2.41}$$

It turns out that the Fourier spectrum of a substitutional structure can be a very intricate object, and that the structure factor $S(Q)$ is in general not a smooth function, but should rather be viewed as a measure, or a generalized function, or distribution. We will come back to this point at the end of this section.

In the sequel we shall be essentially interested in the presence, or the absence, of Bragg peaks, i.e. delta functions, in diffraction spectra. We recall that there is a

Bragg peak at the wavevector Q_0 if the Fourier amplitudes grow proportionally to the numbers of atoms in the samples, i.e.

$$G_n^A(Q_0) \approx C(Q_0)\,\nu_n^A \qquad G_n^B(Q_0) \approx C(Q_0)\,\nu_n^B \qquad n \to \infty \tag{2.42}$$

where the amplitude $C(Q_0)$ is a complex quantity. Equation (2.42) expresses the fact that a macroscopic fraction of the atoms diffract in a coherent way at the wavevector Q_0.

We are thus led to investigate under which conditions the amplitudes given by the recursion relations (2.40) grow according to the law (2.42). Firstly, we observe that this maximal growth takes place for the value $Q = 0$ of the wavevector, where the relations (2.40) are equivalent to the letter counting equations (2.4).

It can be argued that Q_0 is a Bragg wavevector if, and only if, all the phase factors which show up in the recursion relations (2.40) go to unity in the $n \to \infty$ limit, so that the growth is similar to that of the $Q = 0$ case. This argument has been made rigorous by Bombieri and Taylor [4].

In the example of the Fibonacci sequence, the phase factor can be expressed in terms of the Fibonacci numbers, defined in (2.17), and the above condition reads

$$\frac{Q_0 a}{2\pi} F_n \to 0 \qquad \mod 1\,. \tag{2.43}$$

It can be shown in an elementary way (see e.g. [6]) that this condition is fulfilled if, and only if, the wavevector takes the form

$$\frac{Q_0 a}{2\pi} = J + K\tau \tag{2.44}$$

where J and K are two arbitrary integers. Hence the diffraction spectrum of the Fibonacci chain contains Bragg peaks for the values of the wavevector given by (2.44). Those values form a Z-module with rank two, i.e. the set of integer linear combinations of two elementary wavevectors, $2\pi/a$ and $2\pi\tau/a$. As a matter of fact, the whole intensity is concentrated on these Bragg peaks. In other words, we have recovered the well known fact that the Fibonacci chain is quasiperiodic.

Let us now consider an arbitrary substitution σ. The condition that the phase factors converge to unity yields equations of the type

$$x\lambda_1^n \to 0 \qquad \mod 1 \tag{2.45}$$

where λ_1 is the Perron–Frobenius eigenvalue of the substitution matrix. A theorem by Pisot [19]—see also [20] for a detailed exposition—asserts that the limit (2.45) holds true if, and only if

(i) λ_1 is a Pisot number, in the sense defined above,

(ii) x belongs to some Z-module $\mathcal{M}(\lambda_1)$, related to λ_1 in a known fashion.

The general case of quasiperiodic substitutions acting on any finite number of letters is considered in appendix A, where a complete characterization of the associated Fourier module is given. In the present case of binary substitutions and quadratic algebraic integers, we can give an elementary derivation of the module $\mathcal{M}(\lambda_1)$, following the approach described in [6]. Consider a binary

substitution σ with the Pisot property. We can recast the phases which enter the evaluation of the Fourier transform of the structure as follows:

$$Q\ell_n^A \approx Qa(\lambda_1 + \beta - \delta)\Phi_n \qquad Q\ell_n^B \approx Qa(\lambda_1 + \gamma - \alpha)\Phi_n \tag{2.46}$$

where the integers Φ_n have been defined in (2.9), and where exponentially small terms of order λ_2^n have been neglected. We are thus led to study the equation

$$y\Phi_n \to 0 \qquad \text{mod } 1\,. \tag{2.47}$$

Along the lines of [6], we set

$$y\Phi_n = a_n + \delta_n \tag{2.48}$$

with a_n integer, and $|\delta_n| \leqslant \frac{1}{2}$, so that (2.47) is equivalent to $\delta_n \to 0$. The recursion relation (2.9) then implies

$$a_n - sa_{n-1} + pa_{n-2} = -\delta_n + s\delta_{n-1} - p\delta_{n-2} \to 0\,. \tag{2.49}$$

Since the left side of this equation is an integer, it vanishes identically for n large enough. We thus have

$$a_n - sa_{n-1} + pa_{n-2} = 0 \qquad n \geqslant N+2 \tag{2.50}$$

for some finite integer N. This last equation can be solved in a closed form, and yields

$$a_{N+k} = a_N\Phi_{k+1} + (a_{N+1} - sa_N)\Phi_k \qquad k \geqslant 0\,. \tag{2.51}$$

By inserting this result back into (2.48), and taking the $k \to \infty$ limit, we obtain

$$y = \frac{a_{N+1}}{\lambda_1^N} - \frac{pa_N}{\lambda_1^{N+1}}\,. \tag{2.52}$$

We have thus shown that a real number y obeys (2.47) if, and only if, it belongs to the Z-module

$$\mathcal{M}(\lambda_1) = Z\{1, 1/\lambda_1, 1/\lambda_1^2, \ldots\} \tag{2.53}$$

generated by all the negative powers of the Perron–Frobenius eigenvalue. Two different situations have therefore to be considered:

2.4.1. The quasiperiodic case. $\det \mathsf{M} = \pm 1$. In this case, (2.10) implies

$$1/\lambda_1^n = \pm(\Phi_{n+1} - \lambda_1\Phi_n)\,. \tag{2.54}$$

This shows that all the negative powers of λ_1 are integer-linear combinations of 1 and λ_1 itself, so that the module defined in (2.53) coincides with the module over the integers generated by 1 and λ_1: $\mathcal{M}(\lambda_1) = Z\{1, \lambda_1\}$.

The diffraction spectrum has therefore Bragg peaks for the wavevectors Q such that both phases evaluated in (2.46) correspond to y values of the form $y = J + K\lambda_1$. These conditions are met if, and only if

$$\frac{Qa}{2\pi} = M + N\omega \tag{2.55}$$

where M and N are two arbitrary integers. We have introduced the notation

$$\omega = \rho^B = 1 - \rho^A \tag{2.56}$$

where the frequencies ρ^A and ρ^B have been defined in (2.13). The Bragg peaks of the diffraction spectrum are thus located at values of the reduced wavevector $x = Qa/(2\pi)$ which are integer-linear combinations of the frequencies ρ^A and ρ^B. In more technical terms, they are supported by a Z-module with rank two, called the Fourier module. The basis $\{1, \rho^B\}$ of the Fourier module has been chosen in writing (2.55) for the sake of further convenience. We could have chosen other bases as well, such as $\{1, \rho^A\}$ or $\{\rho^A, \rho^B\}$. The result (2.55) generalizes (2.44), obtained in the case of the Fibonacci chain.

For further reference, let us give the formal expressions of the Fourier amplitude $G(Q)$ and of the Fourier intensity $S(Q)$ of the infinite structure

$$\begin{aligned} G(Q) &= \sum_{M,N} C_{M,N}\, \delta\left(\frac{Qa}{2\pi} - M - N\omega\right) \\ S(Q) &= \sum_{M,N} |C_{M,N}|^2\, \delta\left(\frac{Qa}{2\pi} - M - N\omega\right) \end{aligned} \tag{2.57}$$

where the complex Fourier coefficients $C_{M,N}$ are defined as in (2.42).

2.4.2. The limit-quasiperiodic case. $\det \mathsf{M} \neq \pm 1$. Under this condition, all the generators of the module $\mathcal{M}(\lambda_1)$, given in (2.53), are linearly independent over the integers. As a consequence, the Bragg peaks of the diffraction spectrum are supported by a Fourier module which has a countable infinity of generators over the integers. The term 'limit-quasiperiodic' for such a structure has been proposed [22], in analogy with the case of limit-periodic functions, which have a Fourier module with an infinity of generators given by an integer geometrical progression, such as $\mathcal{M}(b) = \{1, 1/b, 1/b^2, \ldots\}$, for some integer base $b \geqslant 2$.

2.5. Summary

To close this section, let us summarize the main results concerning the relationship between the arithmetic properties of a binary substitution σ, and geometrical properties of the associated structure. It turns out that three different cases have to be considered.

Let us emphasize that we have restricted ourselves to substitutions with irreducible characteristic polynomials. Otherwise the situation is more complicated, so that the classification given below has several kinds of exceptions. Interesting examples of such exceptions can be found among the substitutions with constant length [23]. The

associated sequences can also be generated by automata, such as e.g. the Thue–Morse sequence, or the period-doubling sequence.

(a) The non-Pisot case ($|\lambda_2| \geqslant 1$): the extension of the structure in internal space, or equivalently its fluctuations in physical space, diverge as a power law of the system size, with a wandering exponent ζ given in (2.37). The diffraction spectrum does not contain any Bragg peak, except at the origin $Q = 0$ of reciprocal space. There is strong evidence in favour of a singular continuous Fourier intensity measure, in particular from multifractal analysis [7]. The diffraction spectrum usually exhibits a complex pattern of strong singular scattering peaks [9], which possess a simple labelling scheme only in a few specific cases [5,6].

(b) The limit-quasiperiodic case ($|\lambda_2| < 1$, $\det \mathsf{M} = \lambda_1\lambda_2 \neq \pm 1$): the structure exhibits bounded fluctuations with respect to its average lattice, and a bounded extension in internal space. The discrete component of its diffraction spectrum consists in Bragg peaks, supported by a Fourier module with a countable infinity of generators over the integers, related to the negative powers of λ_1. It is most probable that the whole intensity is generically concentrated on this discrete component, so that the structure is almost-periodic, and more precisely 'limit-quasiperiodic' [22]. It could therefore be viewed as a section of a periodic object in some infinite-dimensional (functional) space.

(c) The quasiperiodic case ($\det \mathsf{M} = \lambda_1\lambda_2 = \pm 1$): in this last case, the structure still has bounded fluctuations with respect to its average lattice, and a bounded extension in internal space. The discrete component of its diffraction spectrum consists in Bragg peaks, supported by a Fourier module with rank two, given in 2.55). The whole intensity is concentrated on this discrete component, so that the structure is quasiperiodic. It can therefore be viewed as a section of a periodic object in a two-dimensional superspace, which is the periodic repetition of a bounded atomic surface. Such a description is the central object of the next sections.

3. Binary chains: atomic surfaces

3.1. Definitions

In this section, we study from a general viewpoint the atomic surfaces associated with quasiperiodic binary substitutions. Let σ be such a substitution. We use the notations introduced in section 2, and investigate first the sequence $\{\epsilon_k\}$, defined as

$$\epsilon_k = u_k - u_{k-1} \tag{3.1}$$

where the dimensionless fluctuations u_k have been defined in (2.32). It follows from (3.1) that the ϵ_k assume only two values, namely $\epsilon_k = \epsilon^A$ (respectively, $\epsilon_k = \epsilon^B$), if the kth letter of the sequence Σ is an A (respectively, a B), with

$$\epsilon^A = \rho^B = \omega \qquad \epsilon^B = -\rho^A = \omega - 1\,. \tag{3.2}$$

Let us consider the Fourier amplitude of the sequence $\{\epsilon_k\}$, defined as

$$\tilde{\epsilon}(q) = \sum_k \epsilon_k \, \mathrm{e}^{-\mathrm{i}kq} \tag{3.3}$$

where we have used a lower-case letter for the wavevector q, in order to distinguish the Fourier transform of the abstract sequence from that of the associated atomic structure, considered in section 2. One can show, along the lines of the previous section, that the Fourier amplitude $\tilde{\epsilon}(q)$ consists of Bragg peaks, at wavevectors given by (2.55), with q replacing the product Qa. We thus have

$$\tilde{\epsilon}(q) = \sum_{M,N} c_N \, \delta\left(\frac{q}{2\pi} - M - N\omega\right) . \tag{3.4}$$

The Fourier coefficients depend only on N, since $\tilde{\epsilon}(q)$ is a 2π-periodic (generalized) function of q, whence the notation c_N. Moreover, we have $c_{-N} = c_N^*$, where the star denotes complex conjugation, and

$$c_0 = \langle \epsilon_k \rangle = \lim_{K \to \infty} \frac{1}{K} \sum_{k=1}^{K} \epsilon_k = \rho^A \epsilon^A + \rho^B \epsilon^B = 0 . \tag{3.5}$$

In this last equation, we have introduced the notation $\langle A_k \rangle$ for the spatial average of a sequence $\{A_k\}$ over a sample whose length goes to infinity. This quantity is called a *Cesàro average*.

The sum over the integer N in (3.4) can be interpreted as the Fourier series of a periodic function. We thus obtain

$$\epsilon_k = f(k\omega) \tag{3.6}$$

where

$$f(\theta) = \sum_{N=-\infty}^{+\infty} c_N \, \mathrm{e}^{2\pi \mathrm{i} N \theta} \tag{3.7}$$

is a real periodic function of its argument θ, with unit period. This result means that the binary sequence $\{\epsilon_k\}$, which codes for the letters in the sequence Σ, is given by the restriction of a periodic function $f(\theta)$ of a real variable, to the multiples $\theta = k\omega$ of the 'frequency' ω.

The Fourier coefficients $\{c_N\}$ only depend on the substitution under consideration. One of the goals of the present study is to obtain estimates concerning the decay of the c_N when the label N of the harmonics gets large. It is worth mentioning the Parseval identity

$$\sum_{N=-\infty}^{+\infty} |c_N|^2 = \langle \epsilon_k^2 \rangle = \rho^A (\epsilon^A)^2 + \rho^B (\epsilon^B)^2 = \omega(1-\omega) \tag{3.8}$$

which will be used in the following.

Let us now examine the sequence $\{u_k\}$ of the fluctuations of the atomic positions. By Fourier transforming (3.1), we obtain

$$u_k = g(k\omega) \tag{3.9}$$

where g is still a periodic function, with unit period, given by

$$g(\theta) = \sum_{N=-\infty}^{+\infty} d_N \, \mathrm{e}^{2\pi \mathrm{i} N \theta} . \tag{3.10}$$

The functions f and g are related through

$$f(\theta) = g(\theta) - g(\theta - \omega)\,. \tag{3.11}$$

Equivalently, in terms of their Fourier coefficients d_N and c_N, we have

$$c_N = (1 - e^{-2\pi i N\omega})d_N \qquad N \neq 0 \tag{3.12}$$

whereas d_0 is an irrelevant constant.

The central result (3.9) shows that the fluctuations of the atomic positions with respect to the average lattice are given by the restriction to the multiples of ω of a bounded and 1-periodic function $g(\theta)$, called the *modulation*, or *hull function*.

In the present context, the hull function has a remarkable property. Let us adopt again the initial condition $x_0 = 0$, introduced in last section, and focus our attention on the kth atom of the structure. The result (2.33) implies that the difference between u_k and $k\omega$ is an integer. This observation leads to the following form of the hull function

$$g(\theta) = \theta + m(\theta) \tag{3.13}$$

where $m(\theta)$ is an integer-valued function, so that

$$m(\theta + 1) = m(\theta) - 1\,. \tag{3.14}$$

Consider now the hull function over one period, say $0 \leqslant \theta \leqslant 1$. Since the fluctuations of the atomic abscissas are bounded, the integer-valued function $m(\theta)$ assumes a finite number of values, in a range $m_{\min} \leqslant m(\theta) \leqslant m_{\max}$. The graph of the hull function $g(\theta)$ over one period is therefore contained in a finite number of parallel straight segments with unit slope.

Let S denote the set of the values taken by the hull function $g(\theta)$. The above observation allows us to reconstruct the hull function itself from the very set S, by folding it up modulo its unit period.

It turns out that the set S coincides with the atomic surface of the structure, discussed in the introduction. This important observation is a consequence of the above definitions, especially (2.35). More precisely, if the ratio ξ_0 of bond lengths assumes the fixed-point value (2.24), the physical structure is the intersection of V^{E} with a periodic repetition of the atomic surface S, the latter being a subset of V^{I}. We recall that the length unit in V^{I} has been fixed in (2.31). For a generic value of the ratio ξ_0, the physical structure is not strictly self-similar. This amounts to giving a 'tilt' to the atomic surface S, so that it gets a component in the direction of V^{E}.

3.2. Connection with the projection method

A formal definition of the atomic surface has been given in section 3.1. We now want to illustrate this formalism on the example of structures generated by the standard projection method [24–27]. The atomic surface of such structures is known to be a straight-line segment.

Consider the unit square lattice Z^2 in the two-dimensional plane. The physical space V^{E} is defined as the line with an irrational slope t, passing through the origin. We introduce the notation

$$t = \tan\phi \tag{3.15}$$

with $0 < \phi < \pi/4$, i.e. $0 < t < 1$. An open strip Ω is drawn by sweeping a unit square parallel to V^{E}. This region is therefore defined by the inequalities

$$0 < y - tx < t + 1 . \tag{3.16}$$

Figure 1 illustrates this construction. The structure is defined as the orthogonal projection onto V^{E} of all the lattice points contained in the strip Ω. In other terms, the staircase-shaped broken line considered in the previous section is the only one entirely contained in the open strip Ω, apart from the point at the origin.

We now aim at describing the quasiperiodic structures thus generated by means of the general concepts and notations introduced above. The kth lattice point $\boldsymbol{X}_k$ along the broken line, to the right of the origin, is of the form given by (2.28). On the other hand, its coordinates obey the inequalities (3.16), which express that the point $\boldsymbol{X}_k$ lies in the strip Ω. We thus obtain

$$m^A(k) = k - 1 - \mathrm{Int}(k\omega) \qquad m^B(k) = 1 + \mathrm{Int}(k\omega) \tag{3.17}$$

with the notation

$$\omega = \frac{t}{t+1} = \frac{\sin\phi}{\sin\phi + \cos\phi} . \tag{3.18}$$

Here and throughout the following, $\mathrm{Int}(z)$ and $\mathrm{Frac}(z)$ denote respectively the integer and fractional parts of a real number z:

$$z = \mathrm{Int}(z) + \mathrm{Frac}(z) \qquad 0 \leqslant \mathrm{Frac}(z) < 1 . \tag{3.19}$$

The atomic abscissas x_k can be derived from the result (3.17). We thus obtain a result in agreement with the general expressions (2.32) and (3.9), namely

$$x_k = ka + (\ell^A - \ell^B)\, g(k\omega) \tag{3.20}$$

where the mean interatomic distance a and the bond lengths ℓ^A and ℓ^B read

$$a = \frac{1}{\sin\phi + \cos\phi} \qquad \ell^A = \cos\phi \qquad \ell^B = \sin\phi . \tag{3.21}$$

The functions $f(\theta)$ and $g(\theta)$, introduced in section 3.1, have the following simple forms:

$$g(\theta) = \mathrm{Frac}(\theta) - 1 \tag{3.22}$$

$$f(\theta) = \mathrm{Frac}(\theta) - \mathrm{Frac}(\theta - \omega) = \begin{cases} \omega - 1 & \text{for} \quad 0 < \mathrm{Frac}(\theta) < \omega \\ \omega & \text{for} \quad \mathrm{Frac}(\omega) < \theta < 1 . \end{cases} \tag{3.23}$$

By comparing the explicit form (3.22) of the hull function with the results of section 3.1, we realize that the atomic surface consists of one single interval $S = [-1, 0]$. We have thus recovered the well known description of the

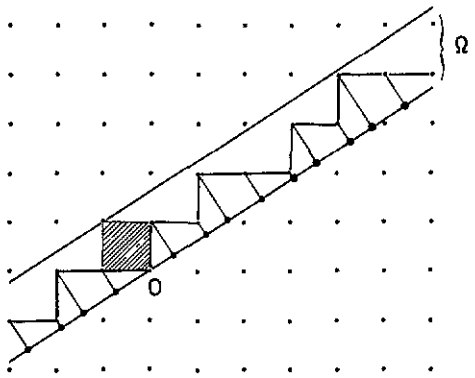

Figure 1. The standard projection method, and the resulting quasiperiodic binary chain.

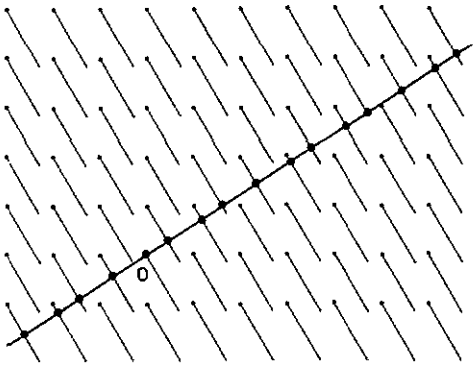

Figure 2. Representation of the standard projection method using atomic surfaces.

standard projection algorithm in terms of atomic surfaces, which is illustrated in figure 2.

The result (3.22)–(3.23) implies that the Fourier coefficients c_N and d_N, introduced in (3.7)–(3.10), read

$$\begin{aligned} &N = 0: \qquad c_0 = 0 \qquad d_0 = -\tfrac{1}{2} \\ &N \neq 0: \qquad c_N = \mathrm{i}(1 - \mathrm{e}^{-2\pi \mathrm{i} N\omega})/(2\pi N) \qquad d_N = \mathrm{i}/(2\pi N)\,. \end{aligned} \tag{3.24}$$

The Parseval formula (3.8) can be checked by means of the identity

$$\sum_{N=1}^{\infty} \frac{1 - \cos(2\pi N\omega)}{N^2} = \pi^2 \omega(1-\omega) \qquad 0 \leqslant \omega \leqslant 1\,. \tag{3.25}$$

The above results hold true for any irrational value of the slope t. When t is a quadratic algebraic integer, the structure generated by the standard projection algorithm is self-similar, and can alternatively be built from a substitution (see [28] for an elementary exposition).

Let us introduce the continued fraction expansion of the slope t

$$t = \cfrac{1}{r_1 + \cfrac{1}{r_2 + \cfrac{1}{r_3 + \cdots}}} = [r_1, r_2, r_3, \ldots] \tag{3.26}$$

where the positive integers $\{r_n\}$ are called the *quotients* associated with the number t.

The binary structure generated by the projection algorithm can be constructed as the limit of a sequence of finite words W_n, which obey the following recursion (concatenation) formulae:

$$W_n = \begin{cases} W_{n-1}^{r_n} W_{n-2} & n \text{ even} \\ W_{n-2} W_{n-1}^{r_n} & n \text{ odd} \end{cases} \tag{3.27}$$

with the initial conditions $W_{-1} = B$ and $W_0 = A$. We have thus $W_1 = BA^{r_1}$, $W_2 = (BA^{r_1})^{r_2}A$, and so on.

When $t = \tan\phi$ is a quadratic irrational number, namely a root of a polynomial equation of degree two, of the form

$$Kt^2 + Lt + M = 0 \tag{3.28}$$

where K, L, and M are three integers, then the quotients $\{r_n\}$ are 'eventually periodic'. This means that there is a period p, such that $r_n = r_{n-p}$ for n large enough, say $n \geqslant n_0$. The recursion formulae (3.27) involve therefore only a finite number of different rules, which can be put together into a single binary substitution.

The matrices of the binary substitutions thus obtained are symmetric, and have unit determinant, in accord with the quasiperiodicity of the structures. Let us mention a simple class of such structures, corresponding to the following quadratic numbers

$$t = [r, r, r, \ldots] = \tfrac{1}{2}(\sqrt{r^2+4} - r) \tag{3.29}$$

where $r \geqslant 1$ is an arbitrary integer. These numbers are often named after metals: $r = 1$ corresponds to the golden mean ($t = \tau^{-1}$) and yields the Fibonacci sequence, whereas $r = 2$ is referred to as the silver mean, and $r = 3$ as the copper mean. The associated substitutions read

$$\sigma_r : \begin{vmatrix} A \to (BA^r)^r A \\ B \to BA^r. \end{vmatrix} \tag{3.30}$$

For $r = 1$, we do not obtain the simple Fibonacci substitution rules (2.14), but their second iterate, which coincides with the substitution σ_1 of (4.2).

3.3. Counting systems associated with substitutions

In this section, we explain how one can associate to a substitution σ a counting system, i.e. a way of counting, or representing, the natural integers in connection with the substitution. This construction, introduced by Dumont [17], holds independently of the Pisot character of the substitution. It has been used especially to prove the result (2.38).

Let σ be a primitive binary substitution, acting on the alphabet $\mathcal{A} = \{A, B\}$, such that $\sigma(A)$ begins with a letter A: we shall say that A is a prefix of $\sigma(A)$. The following proposition holds:

To every integer $k \geqslant 1$ is associated a *unique counting sequence* $(w_i, s_i)_{0 \leqslant i \leqslant n}$, where the w_i are finite words on the alphabet $\mathcal{A}$, and the s_i are letters of that alphabet, so that

(i) The word $w_{i-1}s_{i-1}$ is a prefix of $\sigma(s_i)$, for $1 \leqslant i \leqslant n$;

(ii) The first word is not empty ($w_n \neq \emptyset$), and the word $w_n s_n$ is a prefix of $\sigma(A)$.

The first k letters $\Sigma(k) = \epsilon_1 \ldots \epsilon_k$ of the sequence Σ are given by

$$\Sigma(k) = \sigma^n(w_n)\sigma^{n-1}(w_{n-1}) \cdots \sigma(w_1)w_0. \tag{3.31}$$

As a first example, consider the substitution σ_b, which acts on a single letter A, according to

$$\sigma_b : A \to A^b \tag{3.32}$$

where $b \geqslant 2$ is a given integer. The words of the counting sequence are of the form $w_i = A^{\xi_i}$, with $0 \leqslant \xi_i \leqslant b-1$ for $0 \leqslant i \leqslant n$, and $\xi_n \neq 0$. The representation formula (3.31) implies

$$k = \sum_{i=0}^{n} \xi_i \, b^i \tag{3.33}$$

which is nothing but the usual expansion of the integer k in base b, with digits $\{\xi_i\}$.

The construction described above is a generalization of the concept of counting system to *non-integer bases*. This term comes from the following observation. The number n of 'digits', i.e. of words $\{w_i\}$ employed in the representation of the integer k, obeys the inequalities $\nu_n^A \leqslant k < \nu_{n+1}^A$, which imply the following estimate:

$$n \approx \frac{\ln k}{\ln \lambda_1} \,. \tag{3.34}$$

This demonstrates that the Perron–Frobenius eigenvalue λ_1 of the substitution plays the role of the base b of the counting system.

As a second example, let us come back to the Fibonacci substitution, defined in (2.14). There are only two possibilities for each couple (w_i, s_i) in a counting sequence, namely either $(w_i = \emptyset, s_i = A)$ or $(w_i = A, s_i = B)$. For each integer k, we define a collection of digits $\{\xi_i\}_{0 \leqslant i \leqslant n}$ ($\xi_i = 0$ or 1), as being the lengths of the words w_i. The above construction implies $\xi_n \neq 0$, and $\xi_i = 0$ whenever $\xi_{i-1} = 1$. If $\xi_i = 1$, then $w_i = A$, and $\sigma^i(w_i) = A_i$; if $\xi_i = \emptyset$, then $\sigma^i(w_i) = \emptyset$. The formula (3.31) reads therefore

$$\Sigma(k) = A_n^{\xi_n} A_{n-1}^{\xi_{n-1}} \ldots A_1^{\xi_1} A^{\xi_0} \,. \tag{3.35}$$

In order to make the connection with a counting system more explicit, we notice that the words A_n consist of $\nu_n^A = F_{n+2}$ letters, where the Fibonacci numbers F_n have been introduced in (2.17). As a consequence, (3.35) implies

$$k = \sum_{i=0}^{n} \xi_i F_{i+2} \,. \tag{3.36}$$

Every integer can thus be written in a unique way on the basis of Fibonacci numbers, subjected to the constraints described above. For instance $10 = F_6 + F_3$, and $1992 = F_{17} + F_{14} + F_7 + F_5$.

3.4. Counting systems and atomic surfaces

The purpose of this section is to show how the counting system associated to a substitution, described in the previous section, can be used to derive equations for the corresponding atomic surface S, and to show that S is a self-similar set. The atomic surface has been defined as the set of values taken by the hull function $g(\theta)$. We have equivalently

$$S = \overline{\{u_k\}} \tag{3.37}$$

where the u_k denote the fluctuations of the atomic abscissas, defined in (2.32), and the horizontal bar denotes the topological closure of a set. We also introduce the following subsets of the atomic surface, defined by ascribing values to the last letter s_0 of the counting sequences:

$$\begin{aligned} L^A &= \overline{\{u_k : \ s_0(k) = A\}} \qquad L^B = \overline{\{u_k : \ s_0(k) = B\}} \\ R^A &= \epsilon^A + L^A \qquad R^B = \epsilon^B + L^B \, . \end{aligned} \tag{3.38}$$

As a matter of fact, the letter $s_0(k)$ of the sequence corresponding to the integer k is nothing but ϵ_{k+1}, i.e. the next letter in the sequence. L^A (respectively, L^B) is therefore the part of the atomic surface S restricted to the atomic labels k so that the $(k+1)$th letter is an A (respectively, a B).

In more concrete terms, L^A (respectively, L^B) is the part of the atomic surface describing the *left* extremities of the A bonds (respectively, of the B bonds) of the structure, whereas R^A (respectively, R^B) is the part of the atomic surface describing the *right* extremities of the A bonds (respectively, of the B bonds). We have

$$S = L^A \cup L^B = R^A \cup R^B \, . \tag{3.39}$$

We now arrive at our main point, namely the construction of the atomic surface S by means of the counting theorem mentioned above. We begin by observing that (3.31) can be rewritten as

$$\Sigma(k) = \sigma(\Sigma(k_1))w_0 \qquad \text{with} \qquad \Sigma(k_1) = \sigma^{n-1}(w_n) \cdots \sigma(w_2)w_1 \, . \tag{3.40}$$

This result means that the word $\Sigma(k)$ is the transform by σ of a shorter word $\Sigma(k_1)$, apart from a finite number of last letters, which build the word w_0, and can thus be listed explicitly. The integer k_1 is uniquely defined, since its counting sequence is obtained from that of k by removing the final element (w_0, s_0). This observation leads us to introduce the sets

$$L_1^A = \overline{\{u_k : \ w_0(k) = 0, s_1(k) = A\}} \qquad L_1^B = \overline{\{u_k : \ w_0(k) = 0, s_1(k) = B\}} \tag{3.41}$$

and to proceed along the following lines of reasoning.

- The quantities u_k which are used to define the atomic surface are proportional to the extension of the structure in V^{I}, in units fixed by (2.31). Since the substitution σ acts on V^{I} as a multiplication by λ_2, we have

$$L_1^A = \lambda_2 L^A \qquad L_1^B = \lambda_2 L^B \tag{3.42}$$

  in the sense of pointwise multiplication.
- By keeping track of the different possible values of the final word w_0 in (3.40), we can express the subsets L^A and L^B as sums of translated copies of the rescaled sets L_1^A and L_1^B.

For definiteness, consider again the Fibonacci substitution. The associated counting system has already been described. Table 1 gives the possible values of the couple (w_0, s_0), for each value of s_1. Taking into account all the cases listed

Table 1. Counting system associated with the Fibonacci substitution: possible values of the couple (w_0, s_0), for each value of s_1.

s_1	(w_0, s_0)
A	$(\emptyset, A)$, (A, B)
B	$(\emptyset, A)$

there, and using the values $\omega = \tau^{-2}$, $\lambda_2 = -\tau^{-1}$, we are led to the following self-similarity equations:

$$L^A = (-\tau^{-1}L^A) \cup (-\tau^{-1}L^B) \qquad L^B = \tau^{-2} - \tau^{-1}L^A \tag{3.43}$$

which have for unique solution the intervals

$$L^A = [-\tau^{-2}, \tau^{-3}] \qquad L^B = [\tau^{-3}, \tau^{-1}] \qquad R^A = [0, \tau^{-1}] \qquad R^B = [-\tau^{-2}, 0]\,. \tag{3.44}$$

The atomic surface therefore consists of a single interval $S = [-\tau^{-2}, \tau^{-1}]$, which has unit length. This result is in agreement with those exposed in section 3.2, concerning structures generated by the standard projection algorithm. It is worth recalling that the Fibonacci sequence is equivalent, up to a choice of origin, with that corresponding to the projection method, for a slope $t = \tau^{-1}$.

Let us now turn to the general case. The same procedure yields self-similarity equations, analogous to (3.43), which relate the subsets L^A and L^B to translated copies of the rescaled sets $\lambda_2 L^A$ and $\lambda_2 L^B$. The general form of these equations will be given in (3.49). It can be argued that these formulae determine the sets L^A and L^B in a unique way, since these sets appear as the fixed points of a collection of contracting linear maps.

Such invariant sets have been discussed in the mathematical literature, under the name of 'perfect homogeneous sets' [29,30]. Most mathematical investigations concern the simpler case where the different sets occurring in the right-hand side of (3.49) do not overlap, whereas there is always some overlap in the physical situation of atomic surfaces. It is also worthwhile noticing the close analogy between the present problem and the construction of invariant sets by the so-called 'iterated function systems'—see [31] for an introductory exposition.

We denote by $\theta_+(S)$ and $\theta_-(S)$ the upper and lower extremities of the full atomic surface S, and by $\Delta\theta(S) = \theta_+(S) - \theta_-(S)$ its extension, and we use similar notations for the subsets introduced in (3.38). These quantities are related as follows:

$$\begin{aligned}
&\theta_+(L^B) = \theta_+(R^A) = \theta_+(S) \qquad \theta_+(L^A) = \theta_+(S) - \rho^B \\
&\theta_+(R^B) = \theta_+(S) - \rho^A \qquad \theta_-(L^A) = \theta_-(R^B) = \theta_-(S) \\
&\theta_-(L^B) = \theta_-(S) + \rho^A \qquad \theta_-(R^A) = \theta_-(S) + \rho^B \\
&\Delta\theta(L^A) = \Delta\theta(R^A) = \Delta\theta(S) - \rho^A \qquad \Delta\theta(L^B) = \Delta\theta(R^B) = \Delta\theta(S) - \rho^B\,.
\end{aligned} \tag{3.45}$$

Now consider again the integer-valued function $m(\theta)$, introduced in (3.13). Each interval $[\theta_0, \theta_1]$ where $m(\theta)$ is continuous, and hence constant, contributes to the

atomic surface S for an interval of length $|\theta_1 - \theta_0|$. Let us anticipate that the function $m(\theta)$ only exhibits a countable number of discontinuities. The atomic surface is therefore the union of a countable number of intervals, with a total length equal to unity.

We have thus $\Delta\theta(S) \geqslant 1$, and two cases have to be considered:

(i) $\Delta\theta(S) = 1$. In this first case, the atomic surface S consists of a single unit interval, of the form $S = [s, s+1]$, and the subsets defined above are the following intervals:

$$\begin{aligned} L^A &= [s, s+\rho^A] \qquad L^B = [s+\rho^A, s+1] \\ R^A &= [s+\rho^B, s+1] \qquad R^B = [s, s+\rho^B]\,. \end{aligned} \tag{3.46}$$

We have shown in section 3.2 that the standard projection method yields an atomic surface which is a unit interval. The converse also holds true. Indeed, let $m_0 = \mathrm{Int}(s)$, and $\theta_0 = \mathrm{Frac}(s)$. The hull function then reads

$$g(\theta) = \begin{cases} \theta + m_0 + 1 & \text{for } 0 < \theta < \theta_0 \\ \theta + m_0 & \text{for } \theta_0 < \theta < 1\,. \end{cases} \tag{3.47}$$

This result is equivalent, up to a change of origin, to (3.22), which is characteristic of structures generated by the projection algorithm.

(ii) $\Delta\theta(S) > 1$. In this second case, which is the generic situation among substitutions, the atomic surface has an extension $\Delta\theta(S)$ which is strictly larger than its intrinsic length, or Lebesgue measure, $|S| = 1$. We will show on various examples in section 4 that it usually consists of a countable infinity of disconnected intervals, organized in a self-similar fashion, with a Cantor boundary.

The above construction of atomic surfaces may seem slightly abstract. Therefore, we want to repeat the argument in a more concrete geometric, albeit less rigorous, context, and to derive in another way the formulae of the form (3.43), of which the subsets of the atomic surface are the unique self-similar fixed points. Let P denote the collection of the lattice points $\{X_k\}$, defined in (2.27). Let P^A (respectively, P^B) be the subset of P corresponding to the left extremities of the A bonds (respectively, of the B bonds). The projections of P^A and P^B on the internal space V^1 coincide with the subsets L^A and L^B of the atomic surface S, which have been introduced in (3.38).

The sequence Σ which generates the points $\{X_k\}$ is invariant under the substitution σ. It can therefore also be written in a unique way as a binary sequence, made of the words $A_1 = \sigma(A)$ and $B_1 = \sigma(B)$.

Consider a point X of P, corresponding to the left extremity of a word A_1 (respectively, B_1). Then it is clearly the left extremity of a bond of type a_1 (respectively, b_1), and thus we have $X \in P^{a_1}$ (respectively, $X \in P^{b_1}$). Moreover, there is a point Y in P^A (respectively, in P^B), such that $X = \mathsf{M}Y$. These observations show that we have $\mathsf{M}P^A \subset P^{a_1}$, and $\mathsf{M}P^B \subset P^{b_1}$. The other points X of P do not have a pre-image Y under the transform M. However, they are connected to points which do have such a pre-image, i.e. to points of the sets $\mathsf{M}P^A$ and $\mathsf{M}P^B$, by finite sums of the basis vectors e_1, e_2. These translation vectors can be listed explicitly. The present argument is thus equivalent to the result (3.40).

Let us first take once more, for the sake of definiteness, the example of the Fibonacci sequence. Since we have $A_1 = AB$, $B_1 = A$, three cases have to be considered:

- X is the left extremity of an A bond, the letter A being the first one of a word A_1: such points X describe $\mathsf{M}P^A$, and belong to P^A.
- X is the left extremity of an A bond, the letter A being a word B_1: such points X describe $\mathsf{M}P^B$, and belong to P^A.
- X is the left extremity of a B bond, the letter B being clearly the second one of a word A_1: such points X describe $e_1 + \mathsf{M}P^A$, and belong to P^B.

We thus obtain the equalities

$$P^A = \mathsf{M}P^A \cup \mathsf{M}P^B \qquad P^B = e_1 + \mathsf{M}P^A \,. \tag{3.48}$$

By projecting these formulae onto the internal space V^{I}, where the substitution acts as a multiplication by $\lambda_2 = -\tau^{-1}$, we recover the result (3.43) of the counting system approach.

We end up by giving the self-similarity equations for the atomic surfaces associated with an arbitrary binary substitution. With the notation (2.1), and with $e(A) \equiv e_1$, $e(B) \equiv e_2$, we have

$$\begin{aligned} P^A &= \Big[\bigcup_{i:a_i=A} \Big(\mathsf{M}P^A + \sum_{j<i} e(a_j) \Big) \Big] \cup \Big[\bigcup_{i:b_i=A} \Big(\mathsf{M}P^B + \sum_{j<i} e(b_j) \Big) \Big] \\ P^B &= \Big[\bigcup_{i:a_i=B} \Big(\mathsf{M}P^A + \sum_{j<i} e(a_j) \Big) \Big] \cup \Big[\bigcup_{i:b_i=B} \Big(\mathsf{M}P^B + \sum_{j<i} e(b_j) \Big) \Big] . \end{aligned} \tag{3.49}$$

In order to make the connection with the counting system approach more explicit, consider a point X_k of the set P, and the counting sequence (w_i, s_i) of the associated integer k. Then s_0 (respectively, s_1) indicates whether X_k (respectively, the associated point Y) belongs to P^A or to P^B, whereas w_0 encodes the lattice translation vector leading from $\mathsf{M}Y$ to X.

4. Binary chains: examples

In this section, we present examples of binary substitutions corresponding to quasiperiodic structures which cannot be generated by the projection algorithm, and exhibit complicated atomic surfaces. The dimension of the boundary of the atomic surfaces, and its consequences on the diffraction spectra, will be evaluated in a quantitative way.

4.1. The Fibonacci-squared substitution

As a first example, let us consider all the substitution rules associated with the following matrix:

$$\mathsf{M} = \begin{pmatrix} 2 & 1 \\ 1 & 1 \end{pmatrix} \tag{4.1}$$

which is the square of the matrix (2.15), corresponding to the Fibonacci substitution. The eigenvalues of M read $\lambda_1 = \tau^2$, $\lambda_2 = \tau^{-2}$, where the golden mean τ has been introduced in (2.16). We have $\omega = \tau^{-2}$, with the notation of (2.56).

Table 2. Counting system associated with the Fibonacci-squared substitution σ_3: possible values of the couple (w_0, s_0), for each value of s_1.

s_1	(w_0, s_0)
A	$(\emptyset, A)$, (A, B), (AA, B)
B	$(\emptyset, B)$, (B, A)

Taking into account all the possible orders of the letters in the words $\sigma(A)$ and $\sigma(B)$, we can distinguish six different substitutions corresponding to the matrix **M**, namely

$$\sigma_1 : \begin{vmatrix} A \to BAA \\ B \to BA \end{vmatrix} \qquad \sigma_2 : \begin{vmatrix} A \to ABA \\ B \to BA \end{vmatrix} \qquad \sigma_3 : \begin{vmatrix} A \to AAB \\ B \to BA \end{vmatrix}$$
$$\sigma_4 : \begin{vmatrix} A \to BAA \\ B \to AB \end{vmatrix} \qquad \sigma_5 : \begin{vmatrix} A \to ABA \\ B \to AB \end{vmatrix} \qquad \sigma_6 : \begin{vmatrix} A \to AAB \\ B \to AB . \end{vmatrix} \tag{4.2}$$

Let us first focus our attention onto the substitution σ_3. The associated counting system is described by table 2. According to the procedure of previous section, we can derive from those data the following self-similarity relations between the subsets L^A and L^B of the atomic surface S:

$$\begin{aligned} L^A &= (\tau^{-2} L^A) \cup (\tau^{-2} + \tau^{-2} L^A) \cup (-\tau^{-1} + \tau^{-2} L^B) \\ L^B &= (2\tau^{-2} + \tau^{-2} L^A) \cup (\tau^{-2} L^B) . \end{aligned} \tag{4.3}$$

These equations can be firstly used to determine the extremities $\theta_\pm(L^A)$ and $\theta_\pm(L^B)$. We obtain the following equalities:

$$\begin{aligned} \theta_+(L^A) &= \mathrm{Sup}\ \{\tau^{-2} + \tau^{-2}\theta_+(L^A),\ -\tau^{-1} + \tau^{-2}\theta_+(L^B)\} \\ \theta_-(L^A) &= \mathrm{Inf}\ \{\tau^{-2}\theta_-(L^A),\ -\tau^{-1} + \tau^{-2}\theta_-(L^B)\} \\ \theta_+(L^B) &= \mathrm{Sup}\ \{2\tau^{-2} + \tau^{-2}\theta_+(L^A),\ \tau^{-2}\theta_+(L^B)\} \\ \theta_-(L^B) &= \mathrm{Inf}\ \{2\tau^{-2} + \tau^{-2}\theta_-(L^A),\ \tau^{-2}\theta_-(L^B)\} \end{aligned} \tag{4.4}$$

which have for solution

$$\theta_+(L^A) = \tau^{-1} \qquad \theta_-(L^A) = -\tau^{-1} \qquad \theta_+(L^B) = 1 \qquad \theta_-(L^B) = 0 . \tag{4.5}$$

The extension of the atomic surface therefore reads

$$\Delta\theta(S) = \theta_+(L^B) - \theta_-(L^A) = \tau . \tag{4.6}$$

This quantity is larger than unity, so that a non-trivial structure is expected for the atomic surface.

Figures 3 and 4 present plots of the periodic functions $f(\theta)$ and $g(\theta)$, defined in (3.6) and (3.9). The data are obtained by constructing the finite chain corresponding to the word B_7, which contains $F_{15} = 610$ atoms. The presence of internal structure

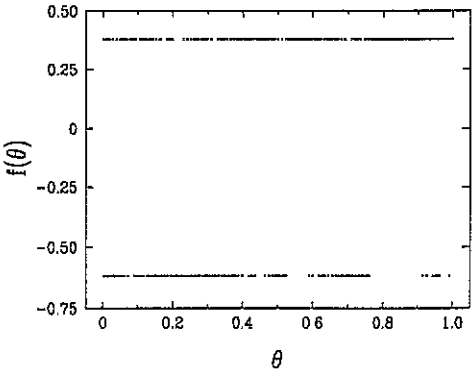

Figure 3. Plot of the function $f(\theta)$ describing the sequence generated by the Fibonacci-squared substitution σ_3.

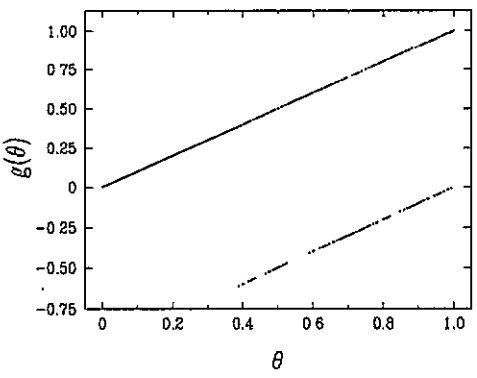

Figure 4. Plot of the modulation function $g(\theta)$ of the Fibonacci-squared substitution σ_3.

in the atomic surface, down to all length scales, is revealed by the very discontinuous nature of the plots, which would be masked by the graphical resolution for larger samples.

The self-similar character of the atomic surface, and the scaling properties of the functions $f(\theta)$ and $g(\theta)$, which can be suspected from the plots, can be derived in a quantitative way from (4.3). Figure 5 illustrates this investigation. The subsets L^A and L^B are symbolically shown as intervals, with extremities given by (4.5), as well as the five sets which enter the right-hand side of (4.3). In the lower part of the plot, the sets are folded modulo the unit period, in order to build the graph of the hull function $g(\theta)$. This function equals $g(\theta) = \theta$ on the set L^B, and on the right half of the set L^A, denoted $L^A_{(2)}$, whereas it equals $g(\theta) = \theta - 1$ on the left half of the set L^A, denoted $L^A_{(1)}$. It turns out that the unit interval gets subdivided in a natural way into $F_7 = 13$ sub-intervals, among which $F_6 = 8$ have length τ^{-5}, and $F_5 = 5$ have length τ^{-6}. The extremities of the subdivisions are labeled as multiples of $\omega = \tau^{-2}$, modulo the unit period: '3' means thus Frac(3ω), '$\bar{5}$' means Frac(-5ω), and so on.

We introduce three functions $a(\theta)$, $b(\theta)$, and $c(\theta)$, defined as being the characteristic functions of the relevant parts, shown on the plot, of the sets L^A or L^B. These functions are equal to unity on the associated sets, and to zero on their complements. We have found it useful to rescale the θ-axis in an appropriate way, so that the functions $a(\theta)$ and $c(\theta)$ are defined on $[0, \tau]$, whereas $b(\theta)$ is defined on $[0, 1]$. The above construction enables one to derive the following functional equations:

$$0 < \theta < \tau: \quad \begin{cases} a(\theta) = a(\tau^{-2}\theta) = c(\tau^{-2}\theta) \\ c(\theta) = c(1 + \tau^{-2}\theta) = 1 - b(\tau^{-2} + \tau^{-2}\theta) \\ c(\theta) - a(\theta) = a(1 + \tau^{-2}\theta) \end{cases} \tag{4.7}$$

$$0 < \theta < 1: \qquad b(\theta) = 1 - b(\tau^{-2}\theta) = a(\tau^{-1} + \tau^{-2}\theta) = c(\tau^{-1} + \tau^{-2}\theta)\,.$$

The structure of the above equations is analogous to that of (B1), (B2), which define a binary Cantor function $\chi(\theta)$ on the unit interval. Inspired by the analysis performed there, and along the lines of the definition (B3), we introduce three elementary partition functions $z_a(s)$, $z_b(s)$, $z_c(s)$, associated with the characteristic

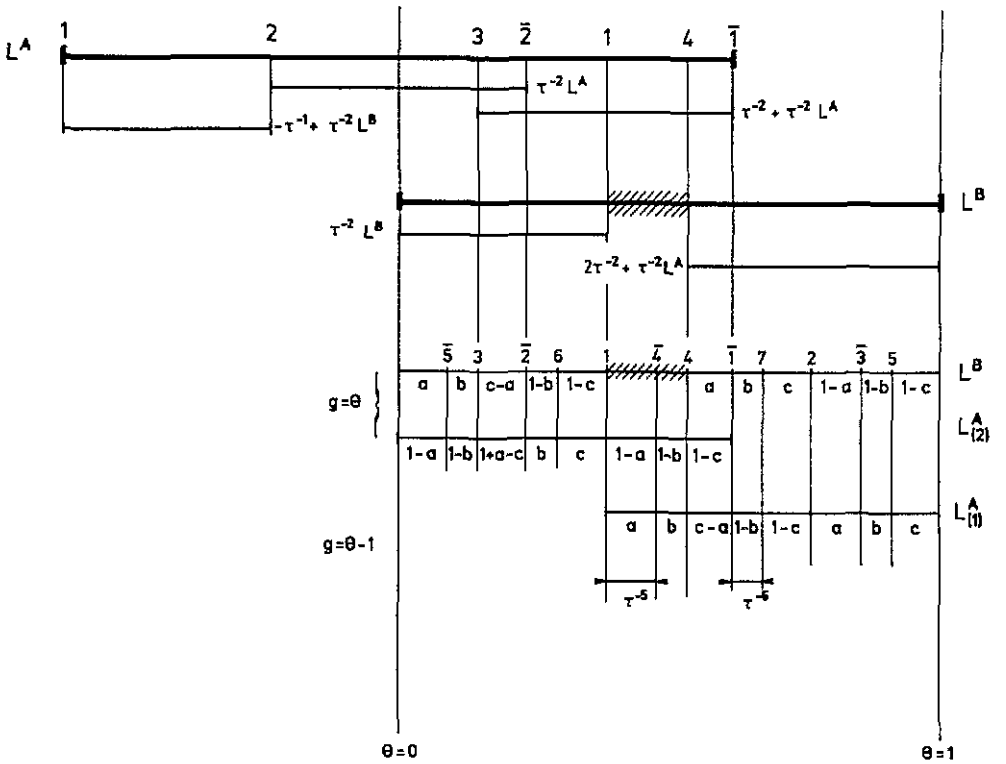

Figure 5. Construction of the modulation function and of the atomic surface associated with the Fibonacci-squared substitution σ_3.

functions defined above. In other words, we set

$$z_a(s) = \sum_j |I_j|^s \,. \tag{4.8}$$

In this definition, the $\{I_j\}$ are all the sub-intervals of $[0, \tau]$ where the characteristic function $a(\theta)$ is a constant (equal either to 1 or to 0), and we use similar definitions for $z_b(s)$ and $z_c(s)$.

We also define the partition function $z_S(s)$ associated with the atomic surface S as

$$z_S(s) = \sum_k |I_k|^s \tag{4.9}$$

where the subintervals $\{I_k\}$ of $[-\tau^{-1}, 1]$ are all the connected components of the atomic surface *and* of its complementary set. We use similar definitions for the partition functions $z_{L^A}(s)$ and $z_{L^B}(s)$, associated with the subsets L^A and L^B. The construction shown in figure 5 implies

$$\begin{aligned} z_S(s) &= \tau^{-2s} + 2\tau^{-4s}\left[z_a(s) + z_b(s) + z_c(s)\right] \\ z_{L^A}(s) &= 2\tau^{-4s}\left[z_a(s) + z_b(s) + z_c(s)\right] \\ z_{L^B}(s) &= \tau^{-4s}\left[z_a(s) + 2z_b(s) + z_c(s) + \tau^{-2s} z_a(s) + 1\right] . \end{aligned} \tag{4.10}$$

On the other hand, the functional equations (4.7) are equivalent to the following identities:

$$\begin{aligned} &\tau^{2s} z_a(s) = z_a(s) + z_b(s) + \tau^{-2s} z_a(s) + 1 \\ &\tau^{2s} z_b(s) = z_a(s) + z_c(s) \qquad \tau^{2s} z_c(s) = z_a(s) + z_b(s) + z_c(s) \end{aligned} \tag{4.11}$$

which have for solution

$$\begin{aligned} &z_a(s) = \frac{\tau^{2s}(\tau^{2s} - 2)}{(\tau^{2s} - 1)(\tau^{4s} - 2\tau^{2s} - 1)} \\ &z_b(s) = \frac{1}{(\tau^{2s} - 1)(\tau^{4s} - 2\tau^{2s} - 1)} \qquad z_c(s) = \frac{1}{\tau^{4s} - 2\tau^{2s} - 1} \end{aligned} \tag{4.12}$$

and hence

$$\begin{aligned} &z_S(s) = \frac{(\tau^{2s} - 1)^2}{\tau^{2s}(\tau^{4s} - 2\tau^{2s} - 1)} \\ &z_{L^A}(s) = \frac{2}{\tau^{2s}(\tau^{4s} - 2\tau^{2s} - 1)} \qquad z_{L^B}(s) = \frac{\tau^{2s} - 1}{\tau^{2s}(\tau^{4s} - 2\tau^{2s} - 1)} . \end{aligned} \tag{4.13}$$

The expressions (4.12), (4.13) for the partition functions agree with the extensions of the associated sets for $s = 1$, as they should, namely $z_a(1) = \tau$, $z_b(1) = 1$, $z_c(1) = \tau$, $z_S(1) = \tau$, $z_{L^A}(1) = 2\tau^{-1}$, and $z_{L^B}(1) = 1$.

The above results diverge under the condition $\tau^{4s} - 2\tau^{2s} - 1 = 0$. The largest real value of s for which this expression vanishes can be used, along the lines of appendix B, to derive the dimension d_B of the boundary of the atomic surface S, namely of the set of its discontinuity points. We thus obtain

$$d_B = \frac{\ln(1 + \sqrt{2})}{2 \ln \tau} = 0.915\,785 . \tag{4.14}$$

This number is very large, namely very close to unity, in accord with the large number of visible discontinuity points in figures 3 and 4.

Let us now examine the consequences on the Fourier transforms of the sequence $\{\epsilon_k\}$ generated by the substitution σ_3, and of the associated structure. Concerning the abstract binary sequence $\{\epsilon_k\}$, we can study the convergence properties of the Parseval identity (3.8). This is indeed a very efficient way of looking at how the intensity is shared among the harmonics. Along the lines of appendix B, we define the quantity

$$\Delta(N) = \omega(1 - \omega) - 2 \sum_{n=1}^{N} |c_n|^2 \tag{4.15}$$

which is expected to exhibit a power-law decay of the form

$$\Delta(N) \approx \frac{1}{N^\eta} \, P\left(\frac{\ln N}{2 \ln \tau}\right) \tag{4.16}$$

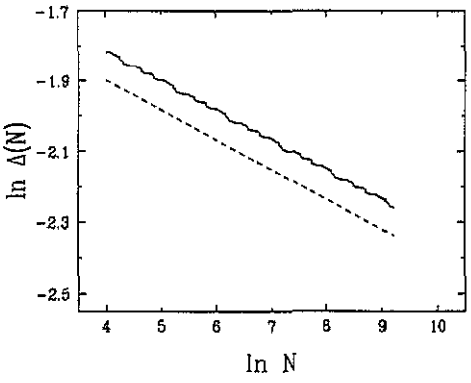

Figure 6. Double logarithmic plot of the quantity $\Delta(N)$, defined in (4.15), showing the anomalous power-law fall-off of Fourier intensities.

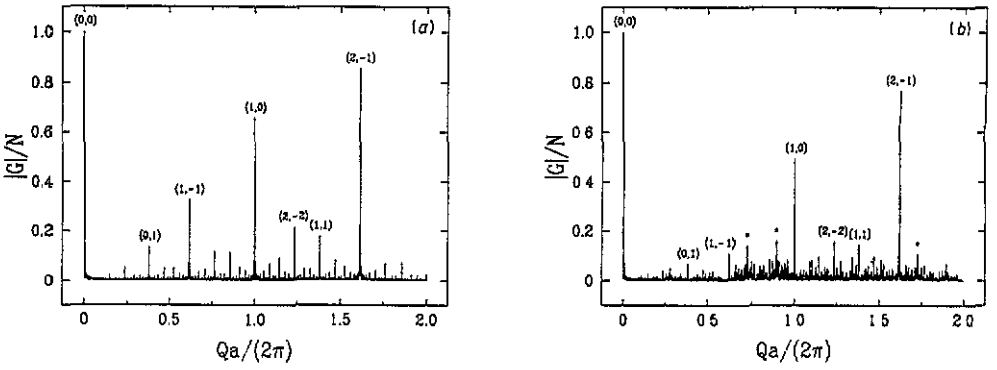

Figure 7. Comparison of the Fourier amplitudes of finite samples, with $F_{16} = 987$ atoms, for (*a*) the Fibonacci chain (smooth atomic surface), and (*b*) the chain generated by the substitution σ_3 (fractal atomic surface).

where the exponent reads $\eta = 1 - d_B = 0.084215$, and where the period of the oscillatory amplitude P is the logarithm of the Perron–Frobenius eigenvalue $\lambda_1 = \tau^2$. Figure 6 presents a log–log plot of $\Delta(N)$, up to $N = 10^4$. The exponent η and the period of the oscillations are found in perfect agreement with the analytic formula (4.16). The present example is a rather extreme one, in the sense that the exponent η is very small. Hence the intensities fall off very slowly: some 44% of the total intensity is still missing by considering 10^4 harmonics!

In order to give a more concrete picture of the physical consequences of the fractal nature of an atomic surface, we compare in figure 7 the Fourier transform of the binary chains generated by (*a*) the Fibonacci substitution, defined in (2.14), and (*b*) the Fibonacci-squared substitution σ_3, defined in (4.2). Both spectra consist of the very same dense set of Bragg peaks. The most clearly visible peaks have been labelled by couples (M, N) of integers, according to (2.55), with $\omega = \tau^{-2}$. Case (*a*) corresponds to a structure generated by the standard projection method, which possesses a smooth atomic surface, whereas case (*b*) is a case of a fractal atomic surface, with a very large boundary dimension, given in (4.14). The difference shows up clearly on the plots. The graph (*b*) exhibits less intense main diffractions, and a more important background noise, induced by the finite sample size ($F_{16} = 987$

atoms in both cases), as well as seemingly peaks, indicated by asterisks, which are actually narrow regions where the maximal visible intensity falls off very slowly.

We end up this section by coming back to all the substitutions which are described by the matrix M of (4.1). The six Fibonacci-squared substitutions, given in (4.2), fall into two classes, according to table 3, which gives the extension $\Delta\theta(S)$ of their atomic surfaces. Four of them $(\sigma_1, \sigma_2, \sigma_5, \sigma_6)$ have $\Delta\theta(S) = 1$. Their atomic surface is therefore an interval, and the associated structures are equivalent to the usual Fibonacci chain, up to different choices of origin. The other two cases (σ_3 and σ_4) are equivalent to each other; σ_3 has been studied at length in this section.

Table 3. Extension of the atomic surface associated with the six variants of the Fibonacci-squared substitution.

Substitution	$\Delta\theta(S)$
$\sigma_1, \sigma_2, \sigma_5, \sigma_6$	1
σ_3, σ_4	$\tau = 1.618034$

4.2. The Fibonacci-cubed substitution

We have shown in the previous section that the nature of the atomic surface is affected by changing the order of the letters in the substitution rules. In the present section, we want to show briefly that interchanging letters in longer substitution rules yields a wider variety of atomic surfaces.

We consider the cube (third power) of the Fibonacci matrix, which reads

$$\mathsf{M} = \begin{pmatrix} 3 & 2 \\ 2 & 1 \end{pmatrix}. \tag{4.17}$$

The associated eigenvalues are $\lambda_1 = \tau^3$, and $\lambda_2 = -\tau^{-3}$. Taking into account the order of letters in the words $\sigma(A)$ and $\sigma(B)$, we distinguish 30 different substitutions corresponding to the matrix M, namely

$$\sigma_1: \begin{cases} A \to BBAAA \\ B \to BAA \end{cases} \quad \sigma_2: \begin{cases} A \to BABAA \\ B \to BAA \end{cases} \quad \sigma_3: \begin{cases} A \to BAABA \\ B \to BAA \end{cases}$$

$$\sigma_4: \begin{cases} A \to BAAAB \\ B \to BAA \end{cases} \quad \sigma_5: \begin{cases} A \to ABBAA \\ B \to BAA \end{cases} \quad \sigma_6: \begin{cases} A \to ABABA \\ B \to BAA \end{cases}$$

$$\sigma_7: \begin{cases} A \to ABAAB \\ B \to BAA \end{cases} \quad \sigma_8: \begin{cases} A \to AABBA \\ B \to BAA \end{cases} \quad \sigma_9: \begin{cases} A \to AABAB \\ B \to BAA \end{cases}$$

$$\sigma_{10}: \begin{cases} A \to AAABB \\ B \to BAA \end{cases} \quad \sigma_{11}: \begin{cases} A \to BBAAA \\ B \to ABA \end{cases} \quad \sigma_{12}: \begin{cases} A \to BABAA \\ B \to ABA \end{cases}$$

$$\sigma_{13}: \begin{cases} A \to BAABA \\ B \to ABA \end{cases} \quad \sigma_{14}: \begin{cases} A \to BAAAB \\ B \to ABA \end{cases} \quad \sigma_{15}: \begin{cases} A \to ABBAA \\ B \to ABA \end{cases}$$

$$\begin{array}{lll}
\sigma_{16}: \begin{vmatrix} A \to ABABA \\ B \to ABA \end{vmatrix} & \sigma_{17}: \begin{vmatrix} A \to ABAAB \\ B \to ABA \end{vmatrix} & \sigma_{18}: \begin{vmatrix} A \to AABBA \\ B \to ABA \end{vmatrix} \\
\sigma_{19}: \begin{vmatrix} A \to AABAB \\ B \to ABA \end{vmatrix} & \sigma_{20}: \begin{vmatrix} A \to AAABB \\ B \to ABA \end{vmatrix} & \sigma_{21}: \begin{vmatrix} A \to BBAAA \\ B \to AAB \end{vmatrix} \\
\sigma_{22}: \begin{vmatrix} A \to BABAA \\ B \to AAB \end{vmatrix} & \sigma_{23}: \begin{vmatrix} A \to BAABA \\ B \to AAB \end{vmatrix} & \sigma_{24}: \begin{vmatrix} A \to BAAAB \\ B \to AAB \end{vmatrix} \\
\sigma_{25}: \begin{vmatrix} A \to ABBAA \\ B \to AAB \end{vmatrix} & \sigma_{26}: \begin{vmatrix} A \to ABABA \\ B \to AAB \end{vmatrix} & \sigma_{27}: \begin{vmatrix} A \to ABAAB \\ B \to AAB \end{vmatrix} \\
\sigma_{28}: \begin{vmatrix} A \to AABBA \\ B \to AAB \end{vmatrix} & \sigma_{29}: \begin{vmatrix} A \to AABAB \\ B \to AAB \end{vmatrix} & \sigma_{30}: \begin{vmatrix} A \to AAABB \\ B \to AAB. \end{vmatrix}
\end{array} \tag{4.18}$$

Table 4. Extension of the atomic surface associated with the 30 variants of the Fibonacci-cubed substitution.

Substitution	$\Delta\theta(S)$
$\sigma_2, \sigma_3, \sigma_{13}, \sigma_{16}, \sigma_{17}, \sigma_{27}, \sigma_{29}$	1
$\sigma_6, \sigma_{12}, \sigma_{19}, \sigma_{26}$	$(\tau+1)/2 = 1.309017$
σ_{14}	$3-\tau = 1.381966$
$\sigma_1, \sigma_4, \sigma_5, \sigma_7, \sigma_{15}, \sigma_{18}, \sigma_{23}, \sigma_{24}, \sigma_{28}, \sigma_{30}$	$\frac{3}{2} = 1.500000$
$\sigma_8, \sigma_9, \sigma_{11}, \sigma_{20}, \sigma_{22}, \sigma_{25}$	$\tau/2+1 = 1.809017$
σ_{10}, σ_{21}	$(\tau+3)/2 = 2.309017$

For each substitution, we have evaluated exactly the extent $\Delta\theta(S)$ of the corresponding atomic surface, by writing and solving formulae analogous to (4.4). The outcomes are summarized in table 4. The 30 variants of the Fibonacci-cubed substitution fall into six inequivalent families, among which the class $\Delta\theta(S) = 1$, corresponding to structures which can be generated by the projection algorithm, and five other classes with fractal atomic surfaces. We notice that four out of the six values of the extent $\Delta\theta(S)$ of the atomic surface are not integer-linear combinations of 1 and τ. The denominator of two comes into the game through the identity $(1+\tau^{-3})^{-1} = \tau/2$. In other words, the end points of the atomic surface S are generally not the projections onto V^1 of superspace lattice points.

5. Ternary chains

This section is devoted to an extension of the previous considerations to chains generated by substitutions acting on any number n of letters. These general considerations will be illustrated by two examples of ternary chains ($n = 3$).

5.1. Generalities

Let σ be a substitution acting on the alphabet $\mathcal{A} = \{A^i (1 \leqslant i \leqslant n)\}$. The associated matrix $\mathbf{M}$ is a square $n \times n$ matrix. We assume that the substitution is quasiperiodic, namely that $\mathbf{M}$ possesses the Pisot property, and that its determinant has unit absolute value. A more detailed set of notations is introduced in appendix A, where the Fourier module of an arbitrary quasiperiodic substitution is derived.

The superspace representation and the construction of atomic surfaces, described in detail in the previous sections in the binary case, can be generalized to any number of letters. Let Σ be a semi-infinite sequence left invariant by σ. We construct a physical structure by putting atoms on a line, at abscissas x_k given by the rule (2.18), where the bond length ℓ_k can take n values ℓ^i, according to the type of the kth letter in the sequence Σ. The frequencies ρ^i of the letter types are given by the components of the normalized right eigenvector v_1 associated with the Perron–Frobenius eigenvalue λ_1. The mean interatomic spacing reads $a = \sum_{i=1}^{n} \ell^i \rho^i$.

The physical structure can be lifted as a broken line drawn on a lattice Z^n, generated by a basis $\{e_i (1 \leqslant i \leqslant n)\}$, in an n-dimensional superspace, $R^n = V^{\mathrm{I}} \oplus V^{\mathrm{E}}$. The physical space V^{E} is spanned by the eigenvector v_1, whereas internal space V^{I} is spanned by the other eigenvectors $\{v_a (2 \leqslant a \leqslant n)\}$. If λ_k and λ_{k+1} are a pair of complex-conjugate eigenvalues, one considers the two-dimensional real eigenspace spanned by the real part, and the imaginary part, of the complex eigenvector v_k. In some cases the action of $\mathbf{M}$ on the lattice Z^n can be viewed as a hyperbolic transformation, leaving invariant a metric tensor, eventually up to a sign [32].

Let us now describe in more detail the modulation function g, and the atomic surface S, associated with the structure. We denote by e_i^{I} and X_k^{I} the projections onto internal space V^{I} of the basis vectors e_i and of the points X_k of the superspace structure. It is shown in appendix A that the Fourier module has rank n, and that it is generated, in reduced units, by the densities ρ^i of the letters A^i in the sequence Σ. As a consequence, the result (3.9) is generalized as

$$X_k^{\mathrm{I}} = g(k\rho^1, \ldots, k\rho^{n-1}) \tag{5.1}$$

where the modulation $g(\theta_1, \ldots, \theta_{n-1})$ is now an $(n-1)$-dimensional vector function. It is periodic, with unit period, in each of the variables θ_i. In other terms, it is a function on the unit $(n-1)$-torus T.

Moreover, by using the identity $\sum_{i=1}^{n} e_i^{\mathrm{I}}, \ \rho^i = 0$, it can be checked that the modulation assumes locally a linear functional form, namely

$$g(\theta_1, \ldots, \theta_{n-1}) = (e_n^{\mathrm{I}} - e_1^{\mathrm{I}})(\theta_1 + m_1) + \cdots + (e_n^{\mathrm{I}} - e_{n-1}^{\mathrm{I}})(\theta_{n-1} + m_{n-1}). \tag{5.2}$$

In this expression, which generalizes (3.13), $m_1, \ldots, m_{n-1}$ are integer functions on T, which are locally constant.

The atomic surface S is defined as (the topological closure in V^{I} of) the set of values taken by the modulation function g on the torus T. The result (5.2) allows one in particular to check that S tessellates V^{I}, i.e. that it is a fundamental domain for the lattice of translations generated by the $(n-1)$ difference vectors $(e_n^{\mathrm{I}} - e_m^{\mathrm{I}})$ $(1 \leqslant m \leqslant n-1)$. This tessellation property is common to all the displacive modulated structures [3, 15]. It implies the physically appealing property that no atom appears or vanishes when the cut is given smooth 'phasonic' deformations around V^{E}.

It turns out that S generically exhibits a fractal boundary, with an anomalous dimension d_B. In the following, we illustrate the above general discussion on the example of ternary chains, generated by substitutions acting on an alphabet made of three letters $\{A, B, C\}$. We shall consider successively one example of each of the two kinds of ternary substitutions, namely one where the substitution matrix has three real eigenvalues, and one with two complex-conjugate eigenvalues.

5.2. One example with real eigenvalues

Our first example is that of a ternary substitution, already discussed in [33], in connection with a quasiperiodic tiling of the plane by three species of triangles, which exhibits a diffraction spectrum with seven-fold rotational symmetry. Consider the following 3×3 substitution matrix:

$$\mathsf{M} = \begin{pmatrix} 1 & 1 & 0 \\ 1 & 0 & 1 \\ 1 & 1 & 1 \end{pmatrix} \tag{5.3}$$

which has for characteristic polynomial $P(\lambda) = \lambda^3 - 2\lambda^2 - \lambda + 1$. The eigenvalues of the substitution matrix M, and the geometrical characteristics of the associated structures, can be expressed in terms of the following three numbers:

$$\begin{aligned} t_1 &= 2\cos(\pi/7) = 1.801\,938 \qquad t_2 = 2\cos(2\pi/7) = 1.246\,980 \\ t_3 &= 2\cos(3\pi/7) = 0.445\,042 \end{aligned} \tag{5.4}$$

which remind us of the seven-fold tiling quoted above. More precisely, the eigenvalues read

$$\begin{aligned} \lambda_1 &= 1 + t_2 = 1/t_3 = t_1 t_2 = t_1^2 - 1 = 2.246\,980 \\ \lambda_2 &= 1 - t_1 = -1/t_2 = -t_1 t_3 = t_3^2 - 1 = -0.801\,938 \\ \lambda_3 &= 1 - t_3 = 1/t_1 = t_2 t_3 = t_2^2 - 1 = 0.554\,958\,. \end{aligned} \tag{5.5}$$

These expressions show that the numbers t_i obey many arithmetical identities, which can be checked by means of their trigonometric expressions (5.4). It is also worth noticing that $\{t_1, -t_2, t_3\}$ are the roots of the polynomial $Q(t) = t^3 - t^2 - 2t + 1$.

The Perron–Frobenius eigenvalue is λ_1, whereas its two conjugates are smaller than unity in absolute value. Moreover we have $\det \mathsf{M} = -1$. The associated structures are therefore quasiperiodic. Taking into account all the possible letter orderings, we consider the following 24 substitution rules:

$$\sigma_1 : \begin{cases} A \to ABC \\ B \to AC \\ C \to BC \end{cases} \qquad \sigma_2 : \begin{cases} A \to ACB \\ B \to AC \\ C \to BC \end{cases} \qquad \sigma_3 : \begin{cases} A \to BAC \\ B \to AC \\ C \to BC \end{cases}$$

$$\sigma_4 : \begin{cases} A \to BCA \\ B \to AC \\ C \to BC \end{cases} \qquad \sigma_5 : \begin{cases} A \to CAB \\ B \to AC \\ C \to BC \end{cases} \qquad \sigma_6 : \begin{cases} A \to CBA \\ B \to AC \\ C \to BC \end{cases}$$

$$
\begin{array}{lll}
\sigma_7: \begin{cases} A \to ABC \\ B \to AC \\ C \to CB \end{cases} & \sigma_8: \begin{cases} A \to ACB \\ B \to AC \\ C \to CB \end{cases} & \sigma_9: \begin{cases} A \to BAC \\ B \to AC \\ C \to CB \end{cases} \\
\sigma_{10}: \begin{cases} A \to BCA \\ B \to AC \\ C \to CB \end{cases} & \sigma_{11}: \begin{cases} A \to CAB \\ B \to AC \\ C \to CB \end{cases} & \sigma_{12}: \begin{cases} A \to CBA \\ B \to AC \\ C \to CB \end{cases} \\
\sigma_{13}: \begin{cases} A \to ABC \\ B \to CA \\ C \to BC \end{cases} & \sigma_{14}: \begin{cases} A \to ACB \\ B \to CA \\ C \to BC \end{cases} & \sigma_{15}: \begin{cases} A \to BAC \\ B \to CA \\ C \to BC \end{cases} \\
\sigma_{16}: \begin{cases} A \to BCA \\ B \to CA \\ C \to BC \end{cases} & \sigma_{17}: \begin{cases} A \to CAB \\ B \to CA \\ C \to BC \end{cases} & \sigma_{18}: \begin{cases} A \to CBA \\ B \to CA \\ C \to BC \end{cases} \\
\sigma_{19}: \begin{cases} A \to ABC \\ B \to CA \\ C \to CB \end{cases} & \sigma_{20}: \begin{cases} A \to ACB \\ B \to CA \\ C \to CB \end{cases} & \sigma_{21}: \begin{cases} A \to BAC \\ B \to CA \\ C \to CB \end{cases} \\
\sigma_{22}: \begin{cases} A \to BCA \\ B \to CA \\ C \to CB \end{cases} & \sigma_{23}: \begin{cases} A \to CAB \\ B \to CA \\ C \to CB \end{cases} & \sigma_{24}: \begin{cases} A \to CBA \\ B \to CA \\ C \to CB\,. \end{cases}
\end{array} \tag{5.6}
$$

Let us choose one of these substitutions, and use it to build an infinite ternary sequence Σ, made of the letters A, B, C. The frequencies of the letter types read

$$\rho^A = t_2 - 1 \qquad \rho^B = 2 - t_2 - t_3 \qquad \rho^C = t_3\,. \tag{5.7}$$

The substitution acts in internal space V^{I} as the following diagonal matrix:

$$\mathsf{M}^{\mathrm{I}} = \begin{pmatrix} \lambda_2 & 0 \\ 0 & \lambda_3 \end{pmatrix} = \begin{pmatrix} 1 - t_1 & 0 \\ 0 & 1 - t_3 \end{pmatrix} \tag{5.8}$$

in the basis of the right eigenvectors v_2 and v_3 of the substitution matrix M. The vectors e_i^{I}, which we denote here by A^{I}, B^{I}, and C^{I}, are given by the components of the corresponding left eigenvectors w_2 and w_3. We choose units so that they assume the simple form

$$A^{\mathrm{I}} = \begin{pmatrix} 1 - t_1 \\ 1 - t_3 \end{pmatrix} \qquad B^{\mathrm{I}} = \begin{pmatrix} t_1^2 \\ t_3^2 \end{pmatrix} \qquad C^{\mathrm{I}} = \begin{pmatrix} -t_1 \\ -t_3 \end{pmatrix}. \tag{5.9}$$

and we denote by (ξ, η) the corresponding Cartesian coordinates.

The atomic surface S tessellates the plane V^{I} under the lattice of translations generated by

$$U = A^{\mathrm{I}} - B^{\mathrm{I}} \qquad V = B^{\mathrm{I}} - C^{\mathrm{I}}\,. \tag{5.10}$$

As a consequence, its area $|S|$ is equal to that of any unit cell of the lattice mentioned above. Assuming, for definiteness, that the basis used to write (5.9) is an orthonormal one, we obtain

$$|S| = |U \times V| = 3t_1 - 1 = 4.405\,813\,. \tag{5.11}$$

This area can alternatively be viewed as that of the projection of the unit cube onto V^{I}, or that of the hexagon spanned by the three vectors defined in (5.9).

The atomic surface exhibits an even wider morphological variety than in the binary case. Figure 8 shows plots of the atomic surface associated with four of the substitutions defined in (5.6). The plots are obtained through a pointwise construction; each of them consists of $\nu_{11}^A = 10\,426$ points. The atomic surface always seems to exhibit a fractal boundary. It is worth noticing that S is not a connected object in the case of the substitution σ_5.

Let us now show how the atomic surface S can be constructed by means of the counting system approach, exposed in section 3.4. For the sake of definiteness, we consider from now on the substitution σ_9, which leads to a rather simple construction for the boundary of the atomic surface. The counting system associated with σ_9 is summarized in table 5. We define the following subsets of the atomic surface: L^A, L^B, L^C, R^A, R^B, R^C, in analogy with the binary case. The results of table 5 imply the following self-similarity relations:

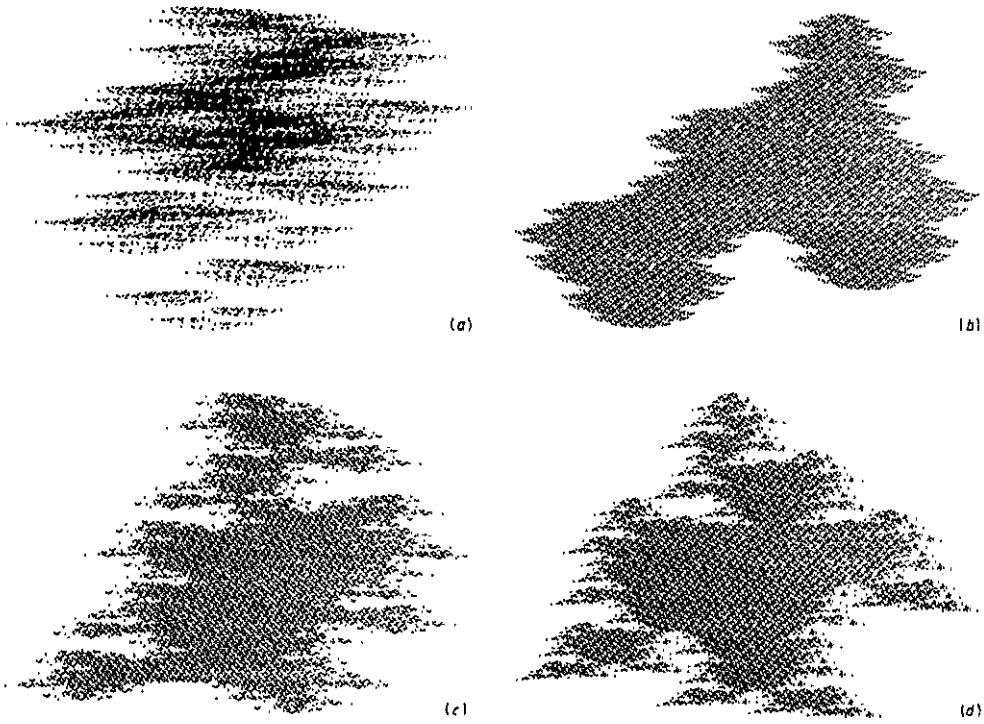

Figure 8. Pointwise plots of the atomic surfaces corresponding to variants of the ternary substitution of (5.6): (*a*) substitution σ_5, (*b*) substitution σ_9, (*c*) substitution σ_{10}, (*d*) substitution σ_{20}.

Table 5. Counting system associated with the ternary substitution σ_9: possible values of the couple (w_0, s_0), for each value of s_1.

s_1	(w_0, s_0)
A	$(\emptyset, B)$, (B, A), (BA, C)
B	$(\emptyset, A)$, (A, C)
C	$(\emptyset, C)$, (C, B)

$$L^A = (B^{\mathrm{I}} + \mathrm{M}^{\mathrm{I}} L^A) \cup (\mathrm{M}^{\mathrm{I}} L^B) \qquad L^B = (\mathrm{M}^{\mathrm{I}} L^A) \cup (C^{\mathrm{I}} + \mathrm{M}^{\mathrm{I}} L^C)$$
$$L^C = (A^{\mathrm{I}} + B^{\mathrm{I}} + \mathrm{M}^{\mathrm{I}} L^A) \cup (A^{\mathrm{I}} + \mathrm{M}^{\mathrm{I}} L^B) \cup (\mathrm{M}^{\mathrm{I}} L^C)\ . \tag{5.12}$$

These equations, which are analogous to (3.43)–(3.49), determine the sets L^A, L^B, L^C, and therefore their union, which is the full atomic surface S. As a first consequence of (5.12), we can determine the upper and lower bounds of these sets along both coordinate axes. We denote by $\xi_\pm(S)$, $\eta_\pm(S)$ these bounds for the full atomic surface S, and use similar notations for its subsets. These quantities obey the following two equations:

$$\xi_+(L^A) = \mathrm{Sup}\,\{t_1^2 + (1-t_1)\xi_-(L^A),\ (1-t_1)\xi_-(L^B)\}$$
$$\xi_-(L^A) = \mathrm{Inf}\,\{t_1^2 + (1-t_1)\xi_+(L^A),\ (1-t_1)\xi_+(L^B)\} \tag{5.13}$$

and ten other ones, which yield

$$\xi_+(L^A) = t_1^2,\ \xi_+(L^B) = 0 \qquad \xi_+(L^C) = t_1^2 - t_1 + 1 \qquad \xi_+(S) = t_1^2$$
$$\xi_-(L^A) = 0 \qquad \xi_-(L^B) = t_1^2 - 5t_1 + 2 \qquad \xi_-(L^C) = t_1^2 - 4t_1 + 2$$
$$\xi_-(S) = t_1^2 - 5t_1 + 2 \qquad \eta_+(L^A) = t_3 \qquad \eta_+(L^B) = -t_3^2 + t_3 \tag{5.14}$$
$$\eta_+(L^C) = 1 \qquad \eta_+(S) = 1 \qquad \eta_-(L^A) = t_3^2 - t_3 \qquad \eta_-(L^B) = -t_3$$
$$\eta_-(L^C) = 0 \qquad \eta_-(S) = -t_3\ .$$

The extension of the atomic surface along both axes therefore reads

$$\Delta\xi(S) = 5t_1 - 2 = 7.009689 \qquad \Delta\eta(S) = t_3 + 1 = 1.445042\ . \tag{5.15}$$

We have repeated this estimation for all substitutions listed in (5.6). The outcomes are given in table 6. There are 11 different classes of substitution rules. We notice the phenomenon already observed in section 4.2, namely the occurrence of an integer denominator, 13 in the present case, in the expression of some of the values of $\Delta\xi(S)$. This denominator shows up via the identity $[1-(1-t_1)^4]^{-1} = (-t_1^2 + 8t_1 + 11)/13$.

Let us now describe how to construct the atomic surface S corresponding to the substitution σ_9, which has already been shown on figure 8(*b*). Figure 9 shows the projection of the unit cube of the lattice Z^3 onto V^{I}, as a hexagon spanned by the vectors defined in (5.9). We recall that this hexagon and the atomic surface have equal areas. Figure 10 shows the polygonal 'skeleton' which will allow us to build the atomic surface and its subsets. The vertices are labelled by the vectors introduced

Table 6. Extension of the atomic surface associated with the 24 variants of the ternary substitution defined in (5.6).

Substitution	$\Delta\xi(S)$	$\Delta\eta(S)$
$\sigma_1, \sigma_3, \sigma_{23}, \sigma_{24}$	$2t_1^2 + 2t_1 - 1 = 9.0978$	1
σ_9, σ_{17}	$5t_1 - 2 = 7.0097$	$t_3 + 1 = 1.4450$
σ_{12}, σ_{13}	$2t_1^2 + 2t_1 - 1 = 9.0978$	$t_3^2 + 1 = 1.1981$
σ_2, σ_{22}	$3t_1^2 + 4t_1 - 2 = 14.9487$	$-t_3^2 + 1 = 0.8019$
σ_{10}, σ_{14}	$(32t_1^2 + 30t_1 - 14)/13 = 11.0740$	$-2t_3 + 2 = 1.1099$
σ_4, σ_{20}	$2t_1^2 + 2t_1 - 1 = 9.0978$	$-t_3^2 - t_3 + 2 = 1.3569$
σ_8, σ_{16}	$3t_1^2 + 3t_1 - 2 = 13.1468$	$t_3^2 + 2t_3 = 1.0881$
σ_6, σ_{19}	$2t_1^2 + 3t_1 - 1 = 10.8998$	$-t_3 + 2 = 1.5550$
σ_7, σ_{18}	$(33t_1^2 + 35t_1 - 12)/13 = 12.1706$	$t_3 + 1 = 1.4450$
σ_{11}, σ_{15}	$3t_1^2 + 3t_1 - 2 = 13.1468$	$t_3^2 + t_3 + 1 = 1.6431$
σ_5, σ_{21}	$2t_1^2 + 6t_1 - 3 = 14.3056$	$-t_3^2 + 2 = 1.8019$

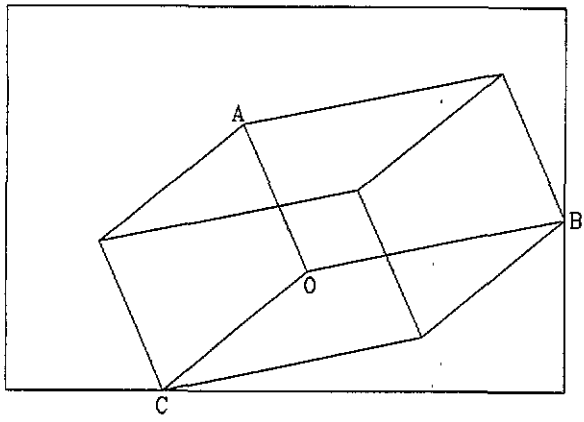

Figure 9. Atomic surface of the substitution σ_9: plot of the projection of the unit superspace cube onto internal space $V^{\perp}$.

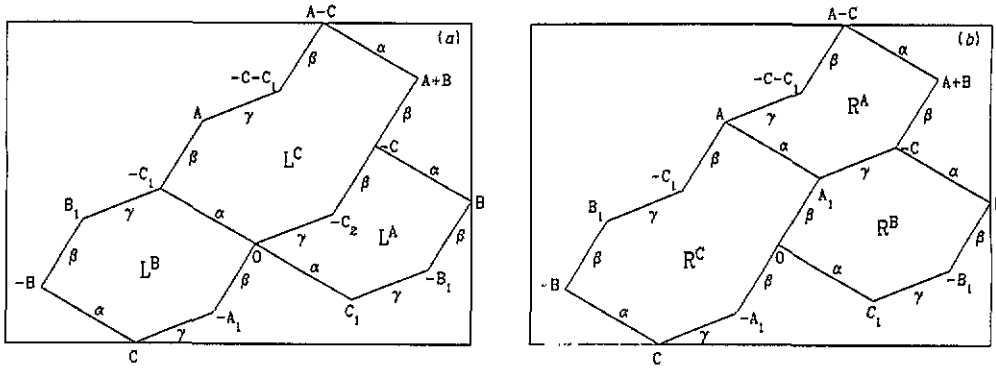

Figure 10. Atomic surface of the substitution σ_9: plot of the polygonal 'skeletons' of (*a*) the subsets L^A, L^B, and L^C, and (*b*) the subsets R^A, R^B, and R^C.

in (5.9), or by their images by the map

$$\mathsf{M}^{\mathrm{I}}: \begin{cases} \boldsymbol{A}^{\mathrm{I}} \to \boldsymbol{A}^{\mathrm{I}} + \boldsymbol{B}^{\mathrm{I}} + \boldsymbol{C}^{\mathrm{I}} \\ \boldsymbol{B}^{\mathrm{I}} \to \boldsymbol{A}^{\mathrm{I}} + \boldsymbol{C}^{\mathrm{I}} \\ \boldsymbol{C}^{\mathrm{I}} \to \boldsymbol{B}^{\mathrm{I}} + \boldsymbol{C}^{\mathrm{I}} \end{cases} \tag{5.16}$$

so that e.g. $\boldsymbol{A}^{\mathrm{I}}_1$ stands for $\mathsf{M}^{\mathrm{I}}(\boldsymbol{A}^{\mathrm{I}})$.

The 14 parts of the boundary of the atomic surface are labelled as three types of arcs, α, β, and γ, spanned respectively by the vectors $\boldsymbol{C}^{\mathrm{I}}$, $\boldsymbol{A}^{\mathrm{I}}$, and $\boldsymbol{C}^{\mathrm{I}}_1$. This labelling is compatible with the partitioning into the subsets L^A, L^B, L^C, R^A, R^B, R^C, and with the tessellation under the translation vectors $\boldsymbol{U}$ and $\boldsymbol{V}$. The self-similarity relations (5.12) imply that the arcs described by the vectors α, β, γ are transformed among themselves by the inverse map $(\mathsf{M}^{\mathrm{I}})^{-1}$, according to

$$(\mathsf{M}^{\mathrm{I}})^{-1}: \begin{cases} \alpha \to -\beta + \gamma \\ \beta \to \beta - \alpha \\ \gamma \to \alpha. \end{cases} \tag{5.17}$$

We have thus obtained an explicit iterative construction rule for the boundary of the atomic surface, and of its relevant subsets.

The result (5.17) shows that $(\mathsf{M}^{\mathrm{I}})^{-1}$ acts as a substitution on the three arcs. The following counting matrix can be associated with it:

$$\boldsymbol{N} = \begin{pmatrix} 0 & 1 & 1 \\ 1 & 1 & 0 \\ 1 & 0 & 0 \end{pmatrix}. \tag{5.18}$$

Its characteristic polynomial reads $Q(x) = x^3 - x^2 - 2x + 1$. Its eigenvalues are therefore the reciprocals of the λ_as, given in (5.5).

The boundary of the atomic surface S and of its subsets is obtained from its skeleton, by applying the transformation (5.17) *ad infinitum*. Figure 11 shows the outcome of this construction. We obtain a fractal boundary, which is self-similar

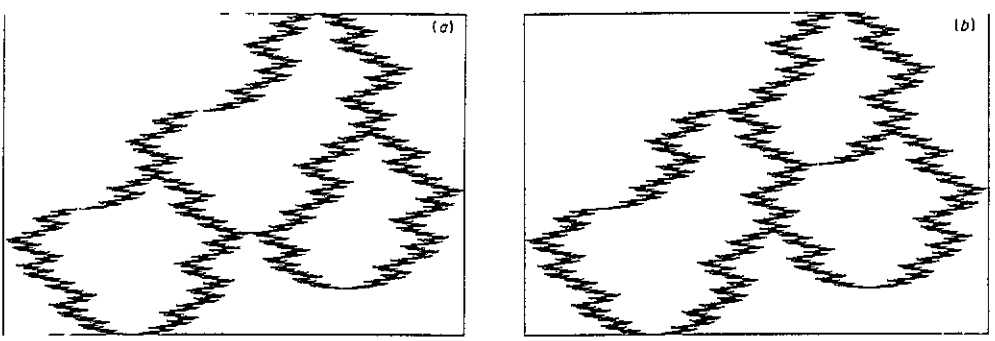

Figure 11. Plot of the fractal boundary of the atomic surface of the substitution σ_9, and of (*a*) the subsets L^A, L^B, and L^C, and (*b*) the subsets R^A, R^B, and R^C.

under the linear transform M^{I}, given in (5.8). It exhibits therefore an anisotropic kind of self-similarity, which can be termed 'self-affinity', although this word has several meanings.

The self-similarity of the boundary of the atomic surface just mentioned above has several kinds of quantitative consequences. Let us first determine its dimension d_{B}. To do so, we observe that, after n iterations of the rules (5.17), the boundary is approximated by a polygon, with a number of sides of order t_1^n. Each side has an extension in the ξ direction of order t_2^{-n}, and an extension in the η direction of order t_1^{-n}. The length of each side is therefore of order t_2^{-n}, and the total length of the boundary of order $(t_1/t_2)^n$, so that the dimension of the boundary reads

$$d_{\mathrm{B}} = \frac{\ln t_1}{\ln t_2} = 2.667\,865\,. \tag{5.19}$$

The above estimates have another consequence, concerning the local scaling behaviour of the boundary of the atomic surface around some special points, which we call 'flat' points. Around such points (ξ_0, η_0), among which all the points marked on figure 10, the equation of the boundary assumes the scaling law

$$|\eta - \eta_0| \sim |\xi - \xi_0|^{d_{\mathrm{B}}}\,. \tag{5.20}$$

5.3. One example with complex eigenvalues

Our second example is based on the following 3×3 substitution matrix:

$$\mathsf{M} = \begin{pmatrix} 0 & 0 & 1 \\ 1 & 0 & 0 \\ 0 & 1 & 1 \end{pmatrix} \tag{5.21}$$

which has for characteristic polynomial $P(\lambda) = \lambda^3 - \lambda^2 - 1$, and for eigenvalues

$$\lambda_1 = 1.465\,571 \qquad \lambda_2 = \lambda_3^* = -0.232\,786 + 0.792\,552\,\mathrm{i}\,. \tag{5.22}$$

The matrix (5.21) has the Pisot property, and its determinant is unity. The associated structures are therefore quasiperiodic.

The interesting new point in the present case, with respect to all examples considered up to now, is the presence of a pair of complex-conjugate subleading eigenvalues, (λ_2, λ_3). The associated left and right eigenvectors have complex components, so that two complex internal eigenspaces show up in a natural way. We choose to denote by V^{I} the complex linear space where the substitution σ acts as a multiplication by the complex number λ_2, i.e. as the similitude composed of the dilatation by a factor $\rho = |\lambda_2| = 0.826\,031$, and of the rotation by an incommensurate angle $\theta = \mathrm{Arg}\ \lambda_2 = 0.295\,468 \times 2\pi$. We use from now on a complex coordinate z in V^{I}, and we choose units so that the internal components of the superspace bonds, which are proportional to the components of w_2, read

$$A^{\mathrm{I}} \equiv z(A) = 1 \qquad B^{\mathrm{I}} \equiv z(B) = \lambda_2 \qquad C^{\mathrm{I}} \equiv z(C) = \lambda_2^2\,. \tag{5.23}$$

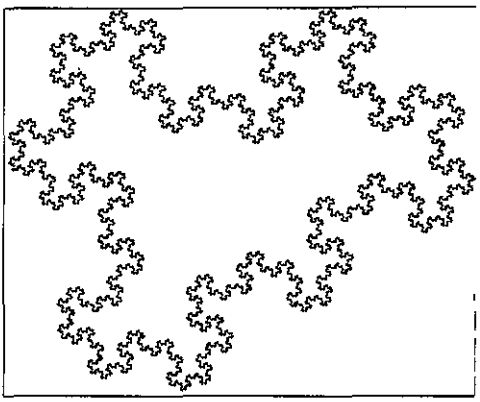

Figure 12. Plot of the fractal boundary of the atomic surface of the ternary substitution defined in (5.24).

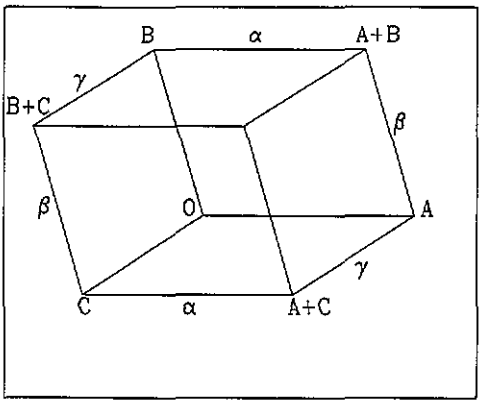

Figure 13. Construction of the fractal boundary shown in figure 12: plot of the projection of the unit superspace cube onto internal space V^{I}.

Let us focus our attention on the following substitution:

$$\sigma : \begin{cases} A \to B \\ B \to C \\ C \to AC \end{cases} \tag{5.24}$$

and on the associated atomic surface. The counting system approach yields the following self-similarity relations:

$$L^A = \lambda_2 L^C \qquad L^B = \lambda_2 L^A \qquad L^C = \lambda_2 L^B \cup \left(z(A) + \lambda_2 L^C\right) \tag{5.25}$$

with $z(A) = 1$, in virtue of the choice of normalization (5.23).

The atomic surface S is the union of the three sets, fixed points of the relations (5.25). Its fractal boundary is shown in figure 12. This closed curve admits an iterative construction, analogous to that exposed in section 5.2. The starting point of the construction is represented on figure 13, which shows the projection onto V^{I} of the unit cube of superspace. Its sides are labelled by three types of arcs, α, β, and γ, spanned respectively by the vectors A^{I}, B^{I}, and C^{I}. These arcs are transformed among themselves by the inverse map $(\mathsf{M}^{\mathrm{I}})^{-1}$, according to

$$(\mathsf{M}^{\mathrm{I}})^{-1} : \begin{cases} \alpha \to -\beta + \gamma \\ \beta \to \alpha \\ \gamma \to \beta \,. \end{cases} \tag{5.26}$$

To the above rules is associated the counting matrix

$$N = \begin{pmatrix} 0 & 1 & 0 \\ 1 & 0 & 1 \\ 1 & 0 & 0 \end{pmatrix} \tag{5.27}$$

which has for characteristic polynomial $Q(x) = x^3 - x + 1$, and for eigenvalues

$$\mu_1 = 1.324\,718 \qquad \mu_2 = \mu_3^* = -0.662\,359 + 0.562\,279\,\mathrm{i}\,. \tag{5.28}$$

It is worthwhile noticing that the eigenvalues μ_a of the counting matrix N are, in the present case, by no means simply related to the eigenvalues λ_a of the substitution matrix $\mathbf{M}$. We end up by giving the expression for the fractal dimension of the boundary of the atomic surface. This quantity can be easily derived by observing that, after n iterations of the rules (5.26), the boundary is approximated by a polygon with a number of sides of order μ_1^n, each side having a length of order $|\lambda_2|^n$. We thus obtain

$$d_B = -\frac{\ln \mu_1}{\ln |\lambda_2|} = 1.471\,305\,. \tag{5.29}$$

The atomic surface of the present example has been recently studied in the mathematical literature [34], as a generalization of the so-called Rauzy fractal, considered in previous works [35,36].

6. Conclusion

Let us first stress that substitutional structures live in their own right, enhancing thus the importance of the real-space approach to the study of aperiodic structures. In this work we have focused our attention on the nature of the atomic surfaces associated with self-similar chains, generated by substitutions. Our position is somewhat analogous to that of experimentalists, who analyse structures in real space, and lift them up in a higher-dimensional superspace, in order to sort out their regularity. In contrast with the latter, we do not start from diffraction spectra to explore superspace properties. We rather use directly the definition of structures in terms of substitutional rules, and draw conclusions concerning, among other aspects, their Fourier transform.

The classes of examples studied here suggest that generic quasiperiodic substitutions correspond to fractal atomic surfaces. The main observable consequence is the anomalously slow fall-off of the intensities of high harmonics, which we have related to the boundary dimension d_B of the atomic surface, at least in the simple case of binary chains. This phenomenon will certainly influence physical properties, such as the width of gaps in electronic spectra, to mention a simple example.

The Pisot nature of a substitution is a *first criterion* which demarcates, among one-dimensional structures, those which possess Bragg peaks from the other ones. The unit determinant condition is a *second criterion*, between quasiperiodic structures, i.e. diffraction spectra which admit a simple indexing scheme, namely n integers, one per superspace coordinate, and those with infinitely many independent Bragg diffractions. Restricting the analysis to quasiperiodic substitutions, the present work emphasizes a *third criterion*, which discriminates between the structures with regular atomic surfaces from those with fractal atomic surfaces. The former ones, such as those generated by the usual projection method, have simpler Fourier spectra than the latter ones, with a faster fall-off of satellite intensities. This criterion amounts, in the binary case, to the computation of the extension $\Delta\theta(S)$ of the atomic surface in internal space. One could have hoped to find a simple way of realizing, by mere inspection of the

substitution rules, whether the associated atomic surface has a fractal or a regular boundary. The present study demonstrates that no such simple criterion exists in general.

The following classification thus emerges for substitutional structures, completing previous studies. As far as long-range translational order is concerned, or equivalently the nature of diffraction spectra, there are three consecutive demarcation lines:

(i) Pisot against non-Pisot structures, i.e. Bragg peaks against continuous Fourier transform;

(ii) among Pisot structures, quasiperiodicity, i.e. a finite-dimensional superspace, against limit-periodicity or limit-quasiperiodicity, i.e. an infinite-dimensional internal space;

(iii) within quasiperiodic structures, smooth atomic surfaces, against atomic surfaces with fractal boundaries.

Going down the above dichotomies, one meets more and more ordered structures, as testified by the 'sharpness' of their diffraction spectra. This progression also goes in the direction of less generic substitutions. Looking in retrospect to the discovery of incommensurate structures, then of quasicrystals, one realizes that nature offers instances of structures which, though highly organized, pertain to increasing levels of complexity. Hence, at least on logical grounds, one might be tempted to imagine that the next class of structures to be discovered with long-range order would be more complex than the previous two cases. Quasiperiodic structures with fractal atomic surfaces represent one plausible step in this direction. They should exhibit a richer diffraction spectrum, with a larger number of visible satellites. This plausibility is strengthened by the fact that, as mentioned in the introduction, the above ideas have been extended to tilings. This will be described in a forthcoming publication.

Acknowledgments

It is a pleasure for us to thank F M Dekking and Z Y Wen for interesting discussions. The Dutch Foundation for Fundamental Research of Matter (FOM) is acknowledged for partial financial support to all four of us.

Appendix A. The Fourier module of a general quasiperiodic substitution

In this appendix we present a self-contained algebraic derivation of the Fourier module associated with an arbitrary quasiperiodic substitution. Let σ be a substitution acting on an alphabet which consists of n letters, $\mathcal{A} = \{A^i \ (1 \leqslant i \leqslant n)\}$. Let $\mathbf{M}$ be the associated matrix. It is an $n \times n$ square matrix, with elements $\mathbf{M}_{i,j}$ positive or zero. We assume the following properties:

(i) The substitution σ is primitive, i.e. all entries of $\mathbf{M}^k$ are strictly positive, for some integer $k \geqslant 1$, so that the Perron–Frobenius theorem holds.

(ii) σ has the Pisot property, which means that, among the n eigenvalues, i.e. the roots of the characteristic polynomial

$$P(\lambda) = \det(\lambda \mathbf{1} - \mathbf{M}) = \lambda^n + s_{n-1}\lambda^{n-1} + \cdots + s_1\lambda + s_0 \qquad \text{(A.1)}$$

the Perron–Frobenius eigenvalue λ_1 is real and larger than unity, whereas the other eigenvalues λ_a $(2 \leqslant a \leqslant n)$ are smaller than unity in modulus.

(iii) $\det \mathsf{M} = \pm 1$.

The above properties imply that the characteristic polynomial is irreducible over the integers, and thus that the Perron–Frobenius eigenvalue is an irrational algebraic integer of degree n, and that the other eigenvalues are its algebraic conjugates. Indeed, if we had $P(\lambda) = R_1(\lambda) R_2(\lambda)$, with polynomials R_a with integer coefficients, each of them would satisfy $R_a(0) = \pm 1$, and thus have at least one root larger than or equal to unity in modulus, in contradiction with the Pisot property.

Let us introduce a few useful notations. We denote by v_1 the right Perron–Frobenius eigenvector, associated with the eigenvalue λ_1, and normalized by the condition

$$\sum_{i=1}^{n} (v_1)_i = 1 . \tag{A.2}$$

The component $(v_1)_i$ represents the frequency ρ^i of the ith letter type A^i in any infinite sequence Σ which is invariant under σ. In a similar way, we denote by w_1 the left Perron–Frobenius eigenvector, normalized so that

$$w_1 \cdot v_1 = \sum_{i=1}^{n} (w_1)_i \, (v_1)_i = 1 . \tag{A.3}$$

The component $(w_1)_i$ represents the bond length ℓ^i associated with the ith letter type A^i, in units of the mean interatomic distance a, under the condition introduced in section 2.1, namely that the physical structure is the projection onto the physical space V^{E} of the superspace lattice points $\{\boldsymbol{X}_k\}$.

We introduce the right and left eigenvectors v_a, w_a corresponding to the other eigenvalues λ_a $(2 \leqslant a \leqslant n)$, by taking the *algebraic conjugate expressions* of the Perron–Frobenius eigenvectors v_1 and w_1 defined above. This means that we replace successively λ_1 by the other eigenvalues λ_a in the expressions for the components $(v_1)_i$ and $(w_1)_i$. This procedure is well defined, since these components are rational functions of λ_1. We have therefore

$$w_a \cdot v_b = \sum_{i=1}^{n} (w_a)_i \, (v_b)_i = \delta_{a,b} \tag{A.4}$$

where $\delta_{a,b}$ is the Kronecker symbol. For $a = b$, (A.4) holds since the conditions (A.2), (A.3) are preserved under algebraic conjugation. For $a \neq b$, (A.4) expresses the well known orthogonality between left and right eigenvectors with different eigenvalues. This property can be proven in an elementary way as follows: $\lambda_a w_a \cdot v_b = (w_a \mathsf{M}) \cdot v_b = w_a \cdot (\mathsf{M} v_b) = \lambda_b w_a \cdot v_b$.

Consider now the matrices P_a $(1 \leqslant a \leqslant n)$, defined by

$$(P_a)_{i,j} = (v_a)_i \, (w_a)_j . \tag{A.5}$$

The identity (A.4) implies

$$P_a v_b = \delta_{a,b} \, v_b \qquad w_b P_a = \delta_{a,b} \, w_b \tag{A.6}$$

and therefore

$$P_a P_b = \delta_{a,b} P_b \qquad \sum_{a=1}^{n} P_a = \mathbf{1}. \tag{A.7}$$

These last equations express that the P_a form a complete set of projectors. Their right (respectively, left) action projects onto the right (respectively, left) eigenspaces of the substitution matrix M.

Let us turn to the analysis of the Fourier transform of the geometrical structures which can be constructed from the substitution σ. We define a reduced wavevector x as follows:

$$Q = \frac{2\pi x}{a}. \tag{A.8}$$

The Fourier module, denoted by $\mathcal{F}$, is defined as the set of values of x corresponding to Bragg peaks. Our aim is to prove that

$$\mathcal{F} = \frac{2\pi}{a} Z\{\rho^i,\ 1 \leqslant i \leqslant n\}. \tag{A.9}$$

This simple and general result means that the Bragg peaks take place at reduced wavevectors x given by integer combinations of the frequencies $\rho^i = (v_1)_i$ of the various letter types.

We now present a lengthy, but self-contained and elementary proof of the fundamental result (A.9). First, we observe, along the lines of [4], and of the analysis of section 2.4, that the reduced wavevector x belongs to $\mathcal{F}$ if, and only if, the phase factors which occur in the recursion relations between Fourier amplitudes go asymptotically to unity. With the notations introduced above, these conditions read

$$x(w_1)_i\ \lambda_1^m \to 0 \mod 1 \qquad m \to \infty \tag{A.10}$$

for $1 \leqslant i \leqslant n$, independently of the choice of the elementary bond lengths ℓ^i. We have therefore to study a set of n equations of the form

$$y\,\lambda_1^m \to 0 \mod 1 \qquad m \to \infty. \tag{A.11}$$

Let us proceed as we did in section 2.4 in the binary case. We introduce the notation

$$T_m = \operatorname{tr} \mathsf{M}^m = \sum_{a=1}^{n} \lambda_a^m. \tag{A.12}$$

The T_m are integers, which obey the following $(n+1)$-term linear recursion relation:

$$T_{m+n} + s_{n-1}T_{m+n-1} + \cdots + s_1 T_{m+1} + s_0 T_m = 0 \tag{A.13}$$

where $s_0, \ldots, s_{n-1}$ are the coefficients of the characteristic polynomial, introduced in (A.1). Then, for each value of y to be considered, we set

$$y\,\lambda_1^m = a_m + \delta_m \tag{A.14}$$

with a_m integer, and $|\delta_m| \leqslant \frac{1}{2}$. Equation (A.11) is then equivalent to the condition $\delta_m \to 0$. The recursion relation (A.13) leads to

$$a_{m+n} - s_{n-1}a_{m+n-1} - \cdots - s_1 a_{m+1} - s_0 a_m$$
$$= -\left(\delta_{m+n} - s_{n-1}\delta_{m+n-1} - \cdots - s_1\delta_{m+1} - s_0\delta_m\right) \to 0. \qquad \text{(A.15)}$$

Since the left side of this last equation is an integer, it vanishes identically for m large enough. We thus have

$$a_{m+n} - s_{n-1}a_{m+n-1} - \cdots - s_1 a_{m+1} - s_0 a_m = 0 \qquad m \geqslant N \qquad \text{(A.16)}$$

for some fixed integer N. Equation (A.16) expresses that the sequence a_{N+m} obeys the linear recursion relation (A.13), and can therefore be expanded on the basis $\{T_{m+k}\ (0 \leqslant k \leqslant n-1)\}$ of solutions of that recursion. We thus obtain

$$a_{N+m} = C_0 T_m + C_1 T_{m+1} + \cdots + C_{n-1} T_{m+n-1} \qquad \text{(A.17)}$$

where the C_k are unknown coefficients. Since the difference between T_m and λ_1^m goes to zero for $m \to \infty$, (A.17) implies

$$y = \lambda_1^{-N}\left(C_0 + C_1\lambda_1 + \cdots + C_{n-1}\lambda_1^{n-1}\right). \qquad \text{(A.18)}$$

The coefficients C_k of the expansion (A.17) are to be determined from the n initial values of the recursion (A.16), i.e. from the following linear system:

$$\begin{cases} a_N & = C_0 T_0 + C_1 T_1 + \cdots + C_{n-1} T_{n-1} \\ a_{N+1} & = C_0 T_1 + C_1 T_2 + \cdots + C_{n-1} T_n \\ & \cdots \\ a_{N+n-1} & = C_0 T_{n-1} + C_1 T_n + \cdots + C_{n-1} T_{2n-2}. \end{cases} \qquad \text{(A.19)}$$

We will not have to solve (A.19) in an explicit form. Let us just notice that its solution is such that the numbers C_k are all rational. The sum between parentheses in the right-hand side of (A.18) belongs therefore to the rational number field $Q(\lambda_1)$ of the Perron–Frobenius eigenvalue λ_1, which is defined as the set of rational linear combinations of the numbers λ_1^k $(0 \leqslant k \leqslant n-1)$.

Moreover, we have $s_0 = (-1)^n \det \mathsf{M} = \pm 1$, so that

$$\frac{1}{\lambda_1} = -s_0\left(\lambda_1^{n-1} + s_{n-1}\lambda_1^{n-2} + \cdots + s_2\lambda_1 + s_1\right). \qquad \text{(A.20)}$$

This relation permits us to show that y also belongs to $Q(\lambda_1)$. Hence the reduced wavevectors x of the Fourier module are among the numbers such that $y = x\,(w_1)_i$ is in the number field $Q(\lambda_1)$, for $1 \leqslant i \leqslant n$. This last statement is equivalent to saying that x itself is in that number field.

There is a rational basis of $Q(\lambda_1)$ which is especially adapted to the present study, namely the set of the n frequencies $\rho^j = (v_1)_j$ of the letter types. Let

$$x = \sum_{j=1}^{n} \xi_j\,(v_1)_j \qquad \text{(A.21)}$$

where the coordinates ξ_j are n rational numbers. We are thus left with the problem of determining for which sets of rational coordinates $\{\xi_j\}$ the n conditions (A.10)

are simultaneously fulfilled. To do so, we notice first that, for x of the form (A.21), the product $x\ (w_1)_i\ \lambda_1^m$ is the term corresponding to $a = 1$ in the following sum:

$$S_{i,m} = \sum_{a=1}^{n} \sum_{j=1}^{n} \xi_j\ (v_a)_j\ (w_a)_i\ \lambda_a^m\ . \tag{A.22}$$

Because of the Pisot property, we thus have $x\ (w_1)_i\ \lambda_1^m \approx S_{i,m}$, up to exponentially small corrections. On the other hand, the sums defined in (A.22) can be evaluated in closed form, by means of the identities (A.5)–(A.7). We thus obtain

$$S_{i,m} = \sum_{j=1}^{n} \xi_j\ (\mathsf{M}^m)_{j,i}\ . \tag{A.23}$$

Since the sums $S_{i,m}$ are integer combinations of the fixed rational numbers $\{\xi_j\}$, the conditions (A.10) amount to requiring that these sums are exactly integers, for m large enough. On the other hand, the ξ_j can be obtained from (A.23) by matrix inversion. They read therefore

$$\xi_j = \sum_{i=1}^{n} (\mathsf{M}^{-m})_{i,j}\ S_{i,m}\ . \tag{A.24}$$

Since the determinant of the substitution matrix is ± 1, the inverse matrix M^{-1} has integer entries. We thus conclude that the coordinates $\{\xi_j\}$ of the reduced Bragg wavevectors in the basis (A.21) are integers. This completes the proof of the result (A.9).

Appendix B. The binary Cantor function

This appendix is devoted to the study of a binary Cantor function $\chi(\theta)$, with the same kind of scaling properties as the characteristic functions associated with the fractal atomic surfaces of binary structures, used in the body of this paper. This Cantor function has the advantage of allowing an explicit analysis.

Let α be a fixed parameter in the range $0 < \alpha < \frac{1}{2}$. The function $\chi(\theta)$ is defined on the unit interval $[0, 1]$ by the following two properties:

$$\chi(\theta) = 1 \qquad \text{for} \qquad \alpha < \theta < 1 - \alpha \tag{B.1}$$

$$\chi(\theta) = 1 - \chi(\alpha\theta) = 1 - \chi(1 - \alpha\theta) \qquad \text{for} \qquad 0 < \theta < 1\ . \tag{B.2}$$

By inserting (B.1) into (B.2), we get $\chi(\theta) = 0$ on both intervals $[\alpha^2, \alpha - \alpha^2]$ and $[1 - \alpha + \alpha^2, 1 - \alpha^2]$. This procedure can be iterated. At the kth iteration, the domain where the function χ is defined is increased by 2^k intervals of length $(1 - 2\alpha)\alpha^k$ each. The limit sum of these lengths equals unity, so that (B.1), (B.2) define a function $\chi(\theta)$, which equals 0 or 1 everywhere, except for a zero-measure set $\mathcal{C}$ of discontinuity points.

Figure B1 shows a plot of the Cantor function $\chi(\theta)$, for $\alpha = 0.4$. It is clear from the construction that $\mathcal{C}$ is a self-similar Cantor set. In order to evaluate its (fractal) dimension, let us introduce the following 'partition function':

$$z(s) = \sum_i |I_i|^s\ . \tag{B.3}$$

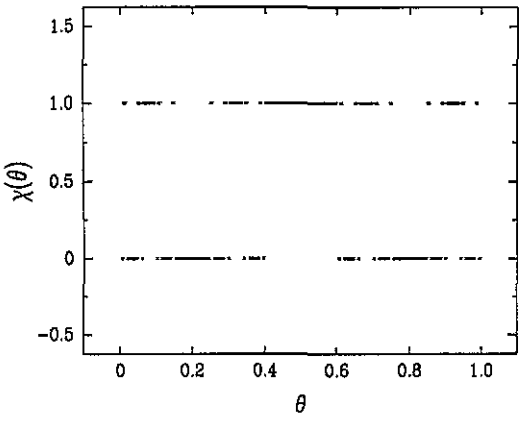

Figure B1. Plot of the Cantor function studied in appendix B, for $\alpha = 0.4$.

In this definition, the sum runs over all intervals on which the function $\chi(\theta)$ is a constant, and $|I_i|$ denotes the length of the interval I_i. The function $z(s)$ is thus the Mellin transform of the length distribution of these intervals. The definition (B.3) implies the normalization $z(s) = 1$, and it is expected to converge for large enough values of the real part of the complex parameter s. The relations (B.1), (B.2) imply the following identity:

$$z(s) = (1-2\alpha)^s + 2\alpha^s z(s) \tag{B.4}$$

which is obtained by writing separately the contribution of the central interval $[\alpha, 1-\alpha]$, and those of both lateral regions. Equation (B.4) yields

$$z(s) = \frac{(1-2\alpha)^s}{1-2\alpha^s}\,. \tag{B.5}$$

The largest real singularity of that expression is to be identified (see e.g. [37]) with the dimension d_B of the set $\mathcal{C}$, which is the boundary of the intervals $\{I_i\}$, whence the notation. We thus obtain

$$d_B = -\frac{\ln 2}{\ln \alpha}\,. \tag{B.6}$$

The dimension d_B increases from zero to unity, as the parameter α is varied from 0 to $\frac{1}{2}$. The result (B.6) could have been derived by more elementary means. Indeed, the graph of the function χ consists, apart from the central interval, of two parts which are similar to the whole graph, reduced by a scaling factor of α. The present approach has the advantage of being systematic; it will be applied to more complex situations in the body of this article.

Let us now turn to the Fourier analysis of the binary Cantor function. We start by extending the function $\chi(\theta)$ to the whole real θ-axis by requiring that it has unit period. It can therefore be represented as a Fourier series of the form

$$\chi(\theta) = \sum_N c_N \, \mathrm{e}^{2\pi i N \theta} \tag{B.7}$$

where the coefficients c_N read

$$c_N = G(2\pi N) \qquad \text{with} \qquad G(q) = \int_0^1 \chi(\theta)\, \mathrm{e}^{-\mathrm{i}q\theta}\, \mathrm{d}\theta\,. \tag{B.8}$$

We can derive from (B.1), (B.2) the following equation for the Fourier transform $G(q)$:

$$G(q) = \frac{1 - e^{-iq}}{iq} - \alpha[1 + e^{-i(1-\alpha)q}]G(\alpha q) . \tag{B.9}$$

The symmetry of the function χ under the exchange of θ into $(1 - \theta)$ suggests that we should set

$$G(q) = e^{-iq/2}H(q) . \tag{B.10}$$

$H(q)$ is then a real and even function, for which (B.9) becomes

$$H(q) = X(q) + Y(q)H(\alpha q) \qquad X(q) = \frac{2}{q}\sin\frac{q}{2} \qquad Y(q) = -2\alpha\cos\frac{(1-\alpha)q}{2} . \tag{B.11}$$

Since $Y(0) = -2\alpha$ is less than unity in absolute value, (B.11) admits the following solution:

$$H(q) = \sum_{n \geqslant 0} X(\alpha^n q) \prod_{0 \leqslant m \leqslant n-1} Y(\alpha^m q) \tag{B.12}$$

which has the convergence properties of a geometrical series.

Let us focus our attention on the behaviour of the Fourier transform for large values of the wavevector q. If the function $\chi(\theta)$ had only one discontinuity point, or a finite number of them, one would observe the simple power laws $G(q) \sim 1/q$, and $c_N \sim 1/N$. In the present case, the binary Cantor function has an infinity of discontinuity points, so that a slower decay can be expected. Let us define the Fourier intensity $S(q)$ through

$$S(q) = |G(q)|^2 = H(q)^2 \tag{B.13}$$

and consider the following integral

$$\Sigma(q) = \int_q^\infty S(p)\,dp . \tag{B.14}$$

The behaviour of this quantity for $q \to \infty$ can be derived from (B.11) in the following way. By squaring both sides of that functional equation, and neglecting the X-function which has a fast decay, as well as interference terms which oscillate rapidly, we obtain

$$\Sigma(q) \approx 2\alpha\ \Sigma(\alpha q) . \tag{B.15}$$

This approximate relation shows that the integrated Fourier intensity obeys the following scaling law for large wavevector:

$$\Sigma(q) \approx \frac{1}{q^\eta} P_1\left(\frac{\ln q}{|\ln \alpha|}\right) \tag{B.16}$$

where the exponent

$$\eta = 1 - d_B = \frac{\ln(2\alpha)}{\ln \alpha} \tag{B.17}$$

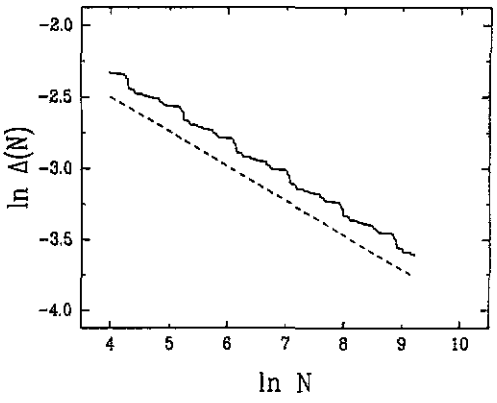

Figure B2. Double logarithmic plot of the quantity $\Delta(N)$, defined in (B.20), showing the anomalous power-law fall-off of Fourier intensities.

is simply related to the boundary dimension d_B, introduced in (B.6). The amplitude P_1 which enters the result (B.16) is a periodic function of its logarithmic argument, with unit period, which reflects the similarity ratio α of the Cantor function in real space.

If the function under study had only finitely many discontinuities, we would have $d_B = 0$, in accord with the laws mentioned above. The more singular the boundary is, the larger its dimension d_B, and the slower the mean decay of its Fourier transform.

An efficient way of viewing the exponent η consists in studying the convergence of the sum involved in the Parseval identity, recalled in (3.8). In the present case, since we have $\chi(\theta) = \chi(\theta)^2$ almost everywhere, the Parseval formula reads

$$\sum_{N=-\infty}^{+\infty} |c_N|^2 = c_0 = \frac{1}{1+2\alpha} . \tag{B.18}$$

Let us introduce the following quantity:

$$\Delta(N) = c_0 - \sum_{n=-N}^{N} |c_n|^2 = \frac{2\alpha}{(1+2\alpha)^2} - 2\sum_{n=1}^{N} |c_n|^2 \tag{B.19}$$

which represents the Fourier intensity which is missed if one considers only the first N harmonics of the Cantor function. The scaling law (B.16) implies that a similar power law holds for $\Delta(N)$, namely

$$\Delta(N) \approx \frac{1}{N^\eta} \, P_2\left(\frac{\ln N}{|\ln \alpha|}\right) . \tag{B.20}$$

This approach will be used in the main body of this paper. It is illustrated on figure B2, which shows a log–log plot of $\Delta(N)$. Both the power law, and the periodic oscillations around it, are found in accord with (B.20).

References

[1] Grünbaum B and G C Shephard 1987 *Tilings and Patterns* (New York: Freeman) ch 10
[2] Janner A and Janssen T 1977 *Phys. Rev.* B 15 643

[3] Janssen T and Janner A 1987 *Adv. Phys.* **36** 519
[4] Bombieri E and Taylor J E 1987 *J. Physique. Coll.* **C3** 19; 1987 *Contemp. Math.* **64** 241
[5] Aubry S, Godrèche C and Luck J M 1987 *Europhys. Lett.* **4** 639
[6] Aubry S, Godrèche C and Luck J M 1988 *J. Stat. Phys.* **51** 1033
[7] Godrèche C and J M Luck 1990 *J. Phys. A: Math. Gen.* **23** 3769
[8] Godrèche C 1991 *Phase Transitions* **32** 45
[9] Godrèche C and Luck J M 1992 *Phys. Rev.* B **45** 176
[10] Bak P 1985 *Phys. Rev.* B **32** 5764; 1986 *Phys. Rev. Lett.* **56** 861
[11] Janssen T 1986 *Acta Cryst.* A **42** 261
[12] Janssen T 1988 *Phys. Rep.* **168** 55
[13] Janssen T 1990 *Proc. Taniguchi Symp.* ed T Fujiwara and T Ogawa (*Springer Series in Solid State Sciences 93*) p 149
[14] Janner A and Janssen T 1990 *Proc. Conf. on Quasicrystals* ed M J Yacaman *et al* (Singapore: World Scientific) p 96
[15] Janssen T and Los J 1991 *Phase Transitions* **32** 29
[16] Gaehler F 1988 *Dissertation* Swiss Federal Institute of Technology, Zurich
[17] Dumont J M 1990 *Number Theory and Physics* ed J M Luck, P Moussa and M Waldschmidt (*Springer Proceedings in Physics 47*) (Berlin: Springer) pp 185–94 and references quoted therein
[18] Bellman R 1970 *Introduction to Matrix Analysis* 2nd edn (New York: McGraw-Hill) ch 16
[19] Pisot C 1938 *Ann. Scuola Norm. Sup. Pisa* **7** 205
[20] Cassels J W S 1957 *An Introduction to Diophantine Approximation* (Cambridge: Cambridge University Press)
[21] Godrèche C, Luck J M and Vallet F 1987 *J. Phys. A: Math. Gen.* **20** 4483
[22] Gaehler F in preparation
[23] Queffélec M 1987 *Substitution Dynamical Systems: Spectral Analysis* (Berlin: Springer) ch 5, 6
[24] de Bruijn N G 1981 *Neder. Akad. Wetensch. Proc.* A **43** 39
[25] Duneau M and Katz A 1985 *Phys. Rev. Lett.* **54** 2688; 1986 *J. Physique* **47** 181
[26] Elser V 1985 *Phys. Rev.* B **32** 4892
[27] Kalugin P A, Kitayev A Yu and Levitov L S 1985 *J. Physique Lett.* **46** L601; 1985 *JETP Lett.* **41** 145
[28] Luck J M and Petritis D 1986 *J. Stat. Phys.* **42** 289
[29] Marion J 1985 *Ann. Inst. Fourier (Grenoble)* **35** 99
[30] Mauldin R D and Williams S C 1986 *Trans. Am. Math. Soc.* **295** 325
[31] Barnsley M 1988 *Fractals Everywhere* (Boston: Academic)
[32] Janner A 1991 *Phys. Rev. Lett.* **67** 2159
[33] Godrèche C and Luck J M 1990 *Proc. Anniversary Adriatico Research Conf. on Quasicrystals* ed M V Jaric and S Lundqvist (Singapore: World Scientific) pp 144–60
[34] Ito S and Kimura M 1991 *Japan. J. Ind. Appl. Math.* **8** #3
[35] Rauzy G 1982 *Bull. Soc. Math. France* **110** 147
[36] Dekking F M 1982 *Adv. Math.* **44** 78; 1982 *J. Comb. Theory* A **32** 315
[37] Feder J 1988 *Fractals* (New York: Plenum)